MYELOID SPECIFIC INHIBITION OF GHS-R MITIGATES EXPERIMENTAL TYPE 2 DIABETES

A Thesis

by

DANIEL VILLARREAL

Submitted to the Office of Graduate and Professional Studies of
Texas A&M University
in partial fulfillment of the requirements for the degree of

MASTER OF SCIENCE

Chair of Committee,	Yuxiang Sun
Committee Members,	Clinton Allred
	James Fluckey
	Shaodong Guo
	Yanan Tian
Head of Department,	Steve Searcy

August 2019

Major Subject: Nutrition

ABSTRACT

Type 2 diabetes is characterized by insulin resistance and beta-cell dysfunction[1]. Macrophages are a major source of inflammatory cytokine IL-1β, which is a major regulator of inflammation in the pancreatic beta-cells [2, 3]. IL-1Ra antagonizes the activity of IL-1β[4]. Beta-cells are the primary source for islet IL-1Ra expression, and IL-1Ra expression in islets diminishes following T2D onset [5]. Ghrelin is nutrient sensor and metabolic regulator. Ghrelin's known receptor is growth hormone secretagogue receptor (GHS-R), reported to govern glucose homeostasis and inflammation under both physiological and pathological conditions[6, 7]. However, little is known of the role of macrophage GHS-R in glycemic regulation of T2D conditions, and its effect on the IL-1Ra:IL-1β ratio is totally unknown. In this study we utilized Western diet + multiple low dose streptozotocin to generate an experimental T2D model to evaluate the effects of myeloid-specific inhibition of GHS-R (LysM-Cre;Ghsr$^{f/f}$). We determined that the WD/STZ model emulated the natural pathogenesis of T2D, the severity of which was attenuated in LysM-Cre;Ghsr$^{f/f}$ mice. We detected attenuated hyperglycemia, increased circulating insulin, reduced glucagon, improved hepatic glucose production, and improved glucose tolerance *in vivo*; as well as enhanced insulin secretion *ex vivo*. Furthermore, gene expression of whole islets exhibited increased insulin signaling genes and an increased ratio of IL-1Ra:IL-1β, suggesting increased IL-1Ra activity. In conclusion, myeloid-specific inhibition of GHS-R mitigated the severity of T2D via improvements of

regulation of glucoregulatory hormones, hepatic glucose metabolism, and islet insulin signaling, at least in part due to increased IL-1Ra activity.

DEDICATION

Dedicated to my Mom and Dad, who've always supported, loved, and worked to provide a better life for their children.

To my beautiful fiancée, I could not have made it through this without your love, encouragement, and smile; I love you.

ACKNOWLEDGEMENTS

I would like to thank my committee chair, Dr. Yuxiang Sun, and my committee members, Dr. Allred, Dr. Fluckey, Dr. Guo, and Dr. Tian, for their guidance and support throughout the course of this research.

Thanks also go to my friends and colleagues in Dr. Sun's lab, and the faculty and staff in NFSC for making my time at Texas A&M University a great experience.

CONTRIBUTORS AND FUNDING SOURCES

Contributors

This work was supervised by a thesis committee members consisting of Drs. Yuxiang Sun, Clinton Allred, and Shaodong Guo of the Department of Nutrition and Food Science, Professor Yanan Tian of the Department of Veterinary Physiology and Pharmacology, and Professor James Fluckey of the Department of Health and Kinesiology. Multiplex analysis/set up was done in collaboration with Da Mi Kim of the Department of Nutrition and Food Science (**Fig. 13**).

All other work conducted for the thesis was completed by the student independently.

Funding Sources

This work was also made possible in part by The National Institute of Health under Grant Number [NIH R56DK118334/R01DK118334-A1]. Its contents are solely the responsibility of the authors and do not necessarily represent the official views of the The National Institute of Health.

NOMENCLATURE

T2D	Type 2 diabetes
T1D	Type 1 diabetes
GHS-R	Growth Hormone Secretagogue Receptor
HFD	High-fat diet
VHFD	Very high-fat diet
WD	Western diet
STZ	Streptozotocin
HGP	Hepatic glucose production
GSIS	Glucose-stimulated insulin secretion
HFCS	High fructose corn syrup
IL-1β	Interleukin-1β
IL-1R1	Interleukin -1 Receptor 1
IL-1Ra	Interleukin- 1 Receptor antagonist

TABLE OF CONTENTS

Page

LIST OF FIGURES

Page

CHAPTER I

INTRODUCTION AND LITERATURE REVIEW

Type 2 diabetes (T2D) is a significant problem due to its exponential prevalence and economic impact. An estimated 30.3 million people of all ages had diabetes in 2015 and cost the U.S. $245 billion in 2012 [8]. Like other metabolic diseases, T2D is characterized by chronic, low-grade inflammation [1]. IL-1β is the chief cytokine known to mediate beta-cell disruption and promotes hepatic insulin resistance [2, 9, 10]. Thus, therapies targeting interruption of the IL-1β/IL-1R1 signaling pathway or IL-1β secretion are promising. Macrophages are the primary immune cell involved in T2D and promote their inflammatory effect via IL-1β secretion and other pro-inflammatory cytokines [2, 3]. The high-fat diet/streptozotocin (HFD/STZ) model of T2D induction closely emulates the natural pathogenesis, inflammatory, and metabolic characteristics of T2D [11-20]. GHS-R governs glucose homeostasis and inflammation under physiological and pathological conditions [7, 21, 22]. However, little is known of the role of GHS-R in regulating macrophage-mediated disruption under T2D conditions.

Relevance of inflammation in T2D pathogenesis

T2D is a complex, multifactorial ailment characterized by hyperglycemia-induced via low-grade, chronic inflammation, peripheral insulin resistance (IR), and pancreatic beta-cell dysfunction [1, 23]. Inflammation was first linked with obesity and T2D in the 1950s when increased fibrinogen and acute-phase reactants were shown to be elevated [24, 25]. Since then, epidemiological, molecular, and clinical studies have supported the notion that obesity exhibits low-grade chronic inflammation, amplified by pro-

inflammatory cytokine production originating from activated monocytes and macrophages [26-28]. Studies like Hotamisligil *et al* observed a link between obesity and inflammation, reporting that TNF-α expressed from adipose tissue was linked with insulin resistance [29]. Immuno-neutralization of TNF-α was confirmed to ameliorate insulin resistance in rodents and humans.

The exact mechanism of inflammation initiation in the progression of obesity is still incompletely understood. One possible etiology is the expansion of adipose tissue and the resulting increases of adipocyte hypertrophy, hyperplasia, and hypoxia [28, 29]. Larger adipocytes out-compete for oxygen leading to hypoxia in other regions triggering cell-autonomous inflammatory responses and secretion of pro-inflammatory chemokines and cytokines. These cytokines/chemokines act in a paracrine/autocrine manner to further progress inflammation and insulin resistance in their locality. Furthermore, inflammation signals macrophages/monocytes to infiltrate, thus further instigating inflammation and insulin resistance. Similarly, under obesogenic conditions, increased hepatic deposition of lipids, exposure to FFAs, and systemic inflammatory cytokines can instantiate hepatocyte-autonomous inflammation [4, 28]. Increased adiposity can further activate hepatic resident macrophages, Kupffer cells, to contribute to the inflammatory milieu and induce hepatic insulin resistance, which is considered non-alcoholic fatty liver disease (NAFLD) [29]. Concomitantly, pancreatic beta-cells respond to excessive nutrition via hyperinsulinemia compensation [2, 3]. Hyperglycemia and FFA exposure sometimes referred to as glucolipotoxicity, can promote ER stress, inflammation, and other modes of compensation [30]. This inflammatory response contributes to further pro-inflammatory cytokine

production from the beta-cell that can act in an autocrine manner to increase pro-inflammatory cytokine secretion and insulin resistance. In particular, hyperglycemia induces the expression of IL-1β from beta-cells which is severely increased under T2D and contributes to beta-cell death, diminished insulin secretory capacity, further cytokine production, and macrophage infiltration [1-3, 23, 31].

Despite the pro-inflammatory milieu being tightly connected with insulin resistance and T2D pathogenesis, there is still no consensus on this cause-and-effect relationship. However, due to the nature of the positive feedback loop that exists between inflammatory mediators and insulin resistant target tissues, there exists opportunities to break the cycle. For example, utilization of anti-inflammatory interventions improved insulin sensitivity in those with chronic inflammation [32, 33]. Similarly, attenuation of insulin resistance with insulin sensitizers improves inflammation in T2D and obesity [34-36]. Thus, interventions targeting major mediators of one or the other show promise in reducing the feedback loop.

This state of excess nutrition and dysregulation of inflammatory homeostasis contributes to peripheral insulin resistance, beta-cell dysfunction, and ultimately, a loss of glucose homeostasis [28, 37, 38]. Interleukin-1β (IL-1β) is one such pro-inflammatory cytokine, produced by macrophages, beta-cells, and Kupffer cells, that contributes to this dysregulation and is associated with the pathogenesis of T2D [34, 39-41]. IL-1β signaling is an important aspect of understanding inflammatory propagation and its downstream effects on tissues related to the pathogenesis of T2D

Interleukin-1 function and signaling in liver/beta-cells

The IL-1 family of cytokines consists of 11 proteins encoded by 11 genes and have been established as major mediators of the innate immune system [42]. The three most prominent are IL-1β, IL-1α, and interleukin-1 receptor antagonist (IL-1Ra). All of these, except for IL-1Ra, require posttranslational processing to become biologically active [4]. IL-1β requires cleavage by caspase-1 within the inflammasome multi-protein complex, while IL-1α is only released following destruction of the cellular membrane. Together they play an important role in inflammation and signal key inflammatory pathways involved in disrupting insulin signaling.

Macrophages are integral to the innate immune system and are the primary source for IL-1β/IL-1α production [42]. Their prominence as major mediators of auto-inflammatory diseases is partly due to their ability to induce expression of their own genes, effectively existing in a positive feedback look with their target tissues. Additionally, activation of their signaling pathway promotes the expression of other pro-inflammatory cytokines such as TNF-α, IL-6, IL-8, MCP-1, COX2, IκBα, and MKP-1. Interleukin-1 receptor-1 (IL-1R1), ubiquitously expressed, is the primary receptor for both of these cytokines that promotes expression of target genes via downstream activation of nuclear factor κB (NF-κB) and c-Jun N-terminal protein kinase (JNK). However, the IL-1R1 signaling pathway and its downstream targets are effectively inhibited by IL-1Ra/IL-1R1 interaction. This pathway is present in many important tissues that undergo dysfunction in the pathogenesis of T2D, including adipose, brain, macrophages, skeletal muscle, liver, and pancreatic beta-cells[43, 44].

Two mechanisms through which hepatic insulin resistance can occur are endoplasmic reticulum (ER) stress and inflammation [45]. Briefly, as the necessity for protein folding and secretion surpasses the ER's capacity to fold and promote protein maturation, there is a build-up of unfolded proteins. This triggers the unfolded protein response (UPR), a collection of transmembrane proteins that aid in the clearing or processing of the unfolded proteins. However, if this is insufficient to attenuate the ER stress, then the UPR mechanisms potentiate apoptotic pathways. This includes activation of JNK pathways, a target of IL-1R1 signaling, which is known to suppress insulin signaling via serine phosphorylation of IRS-1. Additionally, inflammatory cytokines can signal through cytokine receptors, including IL-1R1, to potentiate activation of NF-κB and downstream expression of other pro-inflammatory cytokines. Furthermore, the IL-1R1 pathway activates JNK, similar to ER stress, to inhibit insulin signaling via serine phosphorylation of IRS-1. Subsequently, attenuation of insulin receptor substrate-1 (IRS-1) inhibits the activity of Protein kinase B (AKT), which indirectly promotes Forkhead box protein O1 (FOXO1) activity and downstream gluconeogenic enzymes, Phosphoenolpyruvate carboxykinase (PEPCK) and glucose-6-phosphatase (G6Pase) [4, 29, 45, 46]. In short, IL-1R1 and ER stress pathways disrupt insulin signaling in the liver to increase gluconeogenic activity, while leading to increased production of pro-inflammatory cytokines.

Under T2D, the IL-1R1 pathway operates in the pancreatic beta-cell to disrupt the insulin signaling pathway resulting in the reduction of insulin content, GSIS, and beta-cell mass [47]. Activation of IL-1R1 inhibits the insulin signaling pathway via activation of

NF-κB and JNK. NF-κB promotes the expression of other pro-inflammatory cytokines, including IL-1β, and induces beta-cell death [43]. JNK activity attenuates the activity of IRS-1 and its downstream effector AKT, in addition to promoting beta-cell death [43]. AKT is necessary for beta-cell proliferation, survival, GSIS, and inhibits JNK [43, 48]. Additionally, AKT inhibits FOXO1 [46], which promotes FFA-induced beta-cell apoptosis. Activation of AKT promotes expression of pancreatic and duodenal homeobox 1 (PDX1), a key beta-cell gene involved in insulin transcription, GSIS, and glucose uptake [49, 50]. PDX1 potentiates the expression of the *insulin* gene and glucose transporter 2 (GLUT2), key glucose transporter and sensor [50]. PDX1 deficient beta-cells are susceptible to dedifferentiation into alpha cells, commonly seen in T2D [51]. IL-1β signaling is key in propagating the initiation and maintenance of inflammation and insulin signaling impairment in beta-cells and peripheral tissues [38]. In summary, chronic IL-1R1 signaling via activation of NF-κB and JNK pathways disrupts the beta-cell insulin signaling pathway to attenuate cell growth and induce apoptosis, attenuate glucose uptake/sensing, and ultimately dysfunction GSIS.

In regards to the liver and beta-cells, activation of the IL-1R1 pathway can result in the reduction of insulin signaling, improper functionality, and cell death. Taken together, disruption of inflammatory homeostasis interrupts liver and beta-cell function to the extent that glucose and gluco-regulatory hormone homeostasis can no longer be maintained.

Glucose homeostasis, gluco-regulatory hormones, and IL-1β homeostasis

Glucose homeostasis requires a precise, integrated system involving communication from multiple organs. This involves secretion of gluco-regulatory hormones from the pancreas and the concomitant response by the liver to increase or decrease hepatic glucose production (HGP), as well as insulin/glucose uptake in peripheral tissues. As we've mentioned, macrophages and cytokines are involved in this homeostasis.

Insulin resistance, obesity, and T2D all promote polarization of anti-inflammatory macrophages, designated as M2 macrophages, into pro-inflammatory M1 macrophages; coincidentally, weight loss and improved insulin sensitivity preserve this [52]. Macrophages enhance beta-cell proliferation via secretion of anti-inflammatory cytokines like TGF-β and Wnt [52]. Interestingly, *ex vivo* studies report that IL-1β potentiates insulin secretion and beta-cell proliferation at low concentrations [44]. In response to feeding, macrophages acutely secrete IL-1β to promote insulin secretion to attenuate postprandial glucose [53]. The secretion of IL-1β is dependent on the normalization of glycemia and its insulin stimulatory effects are dependent on the expression of beta-cell IL-1R1, furthermore, this interaction accompanies the compensatory response that beta-cells undergo following increased insulin demand. This suggests that IL-1β and other pro-inflammatory cytokines may serve certain physiological roles when cytokine homeostasis is maintained, possibly dependent on macrophage polarization.

However, chronic hyperglycemia potentiates the chronic secretion of IL-1β and the reduction of its antagonist (IL-1Ra), from beta-cells and macrophages, to disrupt GSIS and dysregulate HGP via IR [44, 54, 55]. While macrophages are the primary IL-1β

source, beta-cells are known to secrete it as well and express its receptor (IL-1R1). IL-1R1 is more highly expressed in the beta-cells than in any other tissue [56] and is thus highly sensitive to IL-1β. The initial secretion of IL-1β from beta-cells and tissue-resident macrophages signal further macrophage infiltration and secretion of IL-1β, potentiating a vicious cycle of islet inflammation [23]. Similar to the pathogenesis of inflammation that occurs in adipose tissue of obese individuals [29].

Similar to adipose tissue inflammation [37], blockade of pro-inflammatory production or the IL-1β feedback loop shows promise in attenuating inflammatory disease. Strategies include targeting IL-1β production from macrophages, it's target tissues or inhibition of its' signaling pathway via IL-1Ra. Beta-cells are the primary source for islet IL-1Ra expression and diminish following T2D onset[5]. Pre-clinical and clinical trials have reported that IL-1Ra improved glucose homeostasis, insulin secretion, and reduced systemic inflammation [57]. This effect lasted well beyond end of treatment and may be attributed to the interruption of an IL-1β feed-back loop between macrophages and beta-cells [58]. A similar feedback loop exists in the liver as Kupffer cells, tissue-resident macrophages, secrete IL-1β to contribute to hepatic IR[59]. Inhibition of the IL-1β signaling pathway or exposure to IL-1R1 antagonist has been reported to attenuate many of the symptoms of T2D such as impaired GSIS, glucose intolerance, insulin resistance, and cardiovascular complications [3, 60, 61]. This suggests that a "re-balancing" of the IL-1β: IL-1Ra ratio may ameliorate the symptoms of chronic IL-1β

These strategies, while promising, do not target macrophage production of IL-1β, only its binding site. Thus, strategies seeking to rebalance IL-1β homeostasis, by

attenuating macrophage production, may effectively alleviate the disruption of glucose metabolism and glucoregulatory hormones.

Ghrelin/GHS-R system

Ghrelin and growth hormone secretagogue receptor (GHS-R) is widely known to influence energy and glucose homeostasis [62-64]. Ghrelin promotes obesity, stimulates appetite, induces insulin resistance, and inhibits insulin secretion [64]. Ghrelin referred to as the 'hunger hormone,' is abundantly produced in the gastric mucosa glands at the base of the stomach [64]. GHS-R is the only known receptor to mediate its effects [65]. Although GHS-R is primarily expressed in the brain, it is also expressed to a lesser degree in the peripheral tissues [66]. Furthermore, GHS-R has been reported to exhibit high constitutive activity suggesting an intrinsic influence of certain functions independent of ghrelin signaling[67].

Global GHS-R ablation exhibits lower fasted insulin/glucose [68] and a lean, insulin sensitive, glucose-tolerant phenotype in aged mice [69]. GHS-$R^{-/-}$ mice bred with *ob/ob*, leptin-deficient mice, worsened hyperglycemia, reduced insulin secretion, and did not attenuate insulin resistance in a leptin-deficient environment [63]. However, ghrelin$^{-/-}$; *ob/ob* mice increased insulin secretion and improved glucose levels. Furthermore, GHS-$R^{-/-}$ mice exposed to either HFD or high fructose corn syrup (HFCS) feeding exhibited improvements in glucose tolerance, glucose levels, insulin sensitivity, and attenuated inflammation in key tissues related to T2D [7, 22]. The highest levels of GHS-R expression are restricted to the pituitary and brain [7]. We report peritoneal macrophages express GHS-R at 60% of hypothalamic expression. In response to HFCS feeding, GHS-

$R^{-/-}$ mice exhibited attenuated expression of IL-1β in peritoneal macrophages (PM) and in white adipose tissue (WAT), which was correlated with improved insulin sensitivity in conjunction with attenuated liver steatosis. The process of aging occurs in parallel with the increased susceptibility to obesity, insulin resistance, chronic inflammation, and T2D [70, 71]. Aged GHS-$R^{-/-}$ mice display improvement in glucose tolerance, insulin sensitivity, and an attenuation of inflammatory cytokines in multiple tissues [69]. WAT, PM, and brown adipose tissue (BAT) exhibited reductions in IL-1β expression, in addition to 264.7 cells cultured with GHS-R antagonist and LPS. Additionally, IL-1β expression is reduced in bone marrow-derived macrophages (BMDM) treated with LPS and GHS-R antagonist (JMV) compared to LPS controls.

We have generated a myeloid-specific GHS-R knockout mouse model (*LysM-Cre; Ghsr*$^{f/f}$), and studied its role in macrophage polarization and find that glucose/insulin levels and glucose/insulin tolerance in unchallenged mice are subtle. Indeed, it seems that GHS-R ablation exhibits an anti-inflammatory phenotype under conditions that produce dysregulation of glucose and inflammatory homeostasis. In summary, GHS-R not only influences energy and glucose homeostasis but may do so via regulation of inflammatory pathways, characterized by improvements in homeostatic functions often impaired under T2D. Thus, an investigation into the role of myeloid-specific GHS-R may elicit new interventions in the regulation of glucose and IL-1β homeostasis to treat T2D.

Mouse models of Type 2 Diabetes

As the incidence and prevalence of T2D continue to rise, the use of cost-effective and accurate models of diabetes are of great use to researchers. Mouse models of diabetes

are ideal as they provide a manageable system and insight into biological processes. Most commonly used are genetic models of diabetes like leptin or leptin-receptor deficient models, *ob/ob* and *db/db*, respectively. However, issues with sterility and cost can prevent researchers from conducting rapid experiments with genetic, T2D models. The use of drugs such as streptozotocin (STZ) has often been employed in producing a diabetic state in mice, via the production of reactive oxygen species [72]. The use of HFD is another way to induce, naturally occurring T2D via insulin resistance, beta-cell compensation, and eventual beta-cell dysfunction (insulin deficiency), and finally hyperglycemia[73]. Finally, a combination of HFD and STZ is reported to closely replicates the pathogenesis of T2D, as well as the metabolic profile [14].

Streptozotocin-induced models of diabetes

High doses of STZ (>65mg/kg) are highly toxic and selective to beta-cells and induce acute beta-cell death, leading to hyperglycemia [11, 74]. Briefly, STZ enters the beta-cell via GLUT2 to induce DNA alkylation followed by activation of poly (ADP-ribosylation) leading to the reduction of nicotinamide and ATP content [72]. The reduction of these two can impede insulin synthesis and secretion. Additionally, STZ promotes nitric oxide activity to reduce mitochondrial ATP and aconitase, a key enzyme in the Krebs cycle. The inhibition of mitochondrial respiration induces the production of reactive oxygen species like xanthine oxidase, hydrogen peroxide, and others. This damages DNA leading to activation of poly (ADP-ribosylation) and ultimately beta-cell death. The extent of this effect is determined by a multitude of factors, predominantly dose size.

Multiple, low doses of STZ (25-55mg/kg) result in a gradual loss of insulin secretion and beta-cell mass, that works in concert with activated immune cells, notably macrophages, and are suggested to be similar with type 1 diabetes (T1D) pathogenesis, as it occurs in the absence of insulin resistance [13, 18, 19, 74, 75]. This differs from the use of STZ in high doses, which primarily induces its effects via acute toxicity. However, T1D pathogenesis relies on the adaptive immune system rather than the innate immune system that produces T2D. Thus when studying the role of the immune system under T1D, genetic models of spontaneous T1D are preferred to inducible T1D [76]. Overall, chemical models alone are unable to emulate the interplay of genetic and environmental stressors that produce T2D and genetic models can be cost and time prohibitive.

Diet-induced models of diabetes

HFD diet models would be most useful at inducing the natural progression of obesity/insulin resistance and eventual beta-cell dysfunction. The use of western diet models are reported to induce metabolic syndrome to a greater degree than even very high-fat diets (VHFD) containing 60% fat, thus may have a stronger impact on T2D induction[77]. This is due to increased saturated fat, high sucrose, and increased cholesterol content. Obesity and/or chronic nutrition can induce hyperinsulinemia compensation via increased beta-cell hypertrophy, proliferation, neogenesis, and apoptosis inhibition [30]. Prolonged compensation is followed by a myriad of stressors that eventually lead to beta-cell dysfunction, such as glucolipotoxicity, endoplasmic reticulum stress, amyloidal stress, inflammatory stress, and oxidative stress. External to the beta-cell, massive expansion of WAT leads to the production of inflammatory

adipocytokines and non-esterified fatty acids (NEFAs) that elicit paracrine and systemic inflammation via production of IL-1β, TNF-α, and IL-6 [55, 78]. These cytokines, via activation of NF-κB and JNK pathways, elicit the production of more cytokines and stimulate macrophage infiltration/cytokine production [79]. Activation of these pathways can result in beta-cell death. Furthermore, islet amyloid polypeptide aggregates can form due to chronic insulin secretion and have been reported to induce beta-cell toxicity, however, the occurrence of these plaque aggregates are not consistent with the onset of T2D [30]. Due to hyperinsulinemia compensation, ER stress can induce UPR which is known to activate JNK and C/EBP-homologous protein (CHOP); inflammatory cytokines can influence ER-stress via the production of nitric oxide (NO) resulting in beta-cell death [80]. Finally, the dysfunction of mitochondrial respiration exhibits oxidative stress induced by lipid peroxidation, protein oxidation, and DNA damage[30]. A combination of excess free radicals ($\bullet O^-_2$, H_2O_2, other ROS) and low anti-oxidant capacity in beta-cells results in dysfunctional GSIS and beta-cell death. Thus, obesity-induced insulin resistance damages beta-cells in a multitude of ways via increased low-grade chronic inflammation mediated by cytokine-induced NF-κB/JNK activity, ER-stress induced activation of the UPR/JNK activity, and dysfunction of mitochondrial respiration resulting in chronically elevated ROS production. While insulin resistance is the primary driver for beta-cell mass adaptation in obesity, almost 2/3 of obese individuals never achieve T2D status [81], similarly, animal models relying solely on HFD feeding can take months to develop T2D or may not at all [82].

Combination HFD and multiple low-dose STZ models of diabetes

Methods involving diet to induce obesity or insulin resistance and beta-cell dysfunction in a relatively short period of time are of great use. Reed *et al.* first proposed a combination of HFD feeding (40% fat) for 2 weeks to induce insulin resistance, confirmed by similar glucose clearance rates but increased insulin response in HFD-group, and a single dose STZ injection to promote beta-cell dysfunction and subsequent hyperglycemia within a week [17]. This was then adapted using multiple, low dose STZ regimen to better emulate the inflammation-mediated beta-cell dysfunction [83]. Since then many researchers have modified the duration of HFD and the concentration of STZ dose. More recently, Nath *et al.* set out to further improve upon this by measuring lipid profiles, elevated oxidative stress, altered tissue histopathology, and alter glucose metabolism. A very high-fat diet (VHFD) (58%) was used in this study for 3 weeks before 5 doses of 40 mg/kg of STZ, VHFD was discontinued after the last injection. Partial destruction of beta-cells characterized by severely diminished islet mass, using histology, was observed. Increased oxidative stress in liver, kidney, and heart was observed, similar to T2D, as well as reduced anti-oxidant enzyme, catalase. Higher total cholesterol, LDL, VLDL, triglycerides, and lower HDL were recorded in VHFD/STZ treated mice, similar to T2D lipid profiles. Additionally, the HFD/STZ model is reported to simulate late-stage T2D. Early stage T2D can be characterized as exhibiting hyperglycemia in conjunction with relatively high insulin level, however, late-stage T2D exhibit similar or lower levels of insulin compared to healthy individuals[14, 73]. However, exactly how both HFD and low-dose STZ mediate their beta-cell-specific effects is still poorly understood. However,

increased expression of TNF-α, IL-6, and IL-1β have all been reported to be increased within HFD/STZ treated rodents, similar to what is seen in T2D [74]. Whether that effect is mediated via inflammatory or primarily oxidative-stress related is even less understood. It should be noted that due to the inherent complexity and heterogeneity of T2D; animal models of T2D will never be fully representative of human T2D pathogenesis, yet strategies seeking to adhere as closely to the natural progression of T2D are necessary. In any case, many have lauded this model as a cost effective, advantageous model that closely reflects the metabolic profile of late-stage T2D, as well as elicits an immune response [14, 18, 74, 83].

Focus of study

In this study, we hypothesize that GHS-R in myeloid cells impairs insulin secretion and increases glucose production under T2D, possible due to the lack of IL-1Ra in islets (**Fig. 1**). To confirm this we first determined whether the Western diet + multiple low-dose STZ models emulated the pathogenesis of T2D and that LysM-Cre;Ghsr$^{f/f}$ rescues it. To do this we evaluated changes in body weight/composition, and circulating glucose, insulin, glucagon, and calculated HOMA-IR; followed by evaluating whether LysM-Cre;Ghsr$^{f/f}$ attenuated the severity of those parameters. We then determined whether myeloid-specific GHS-R increased glucose production, reduced insulin secretion, downregulated insulin signaling, and exacerbated inflammation under T2D. This was done by assessing metabolic regulation via GTT, PTT, and *ex vivo* GSIS. Finally, we performed gene profile analysis to assess expression levels of IL-1 related genes and insulin signaling pathways in whole islet tissue and measured inflammatory cytokines using a multiplex kit.

Fig. 1

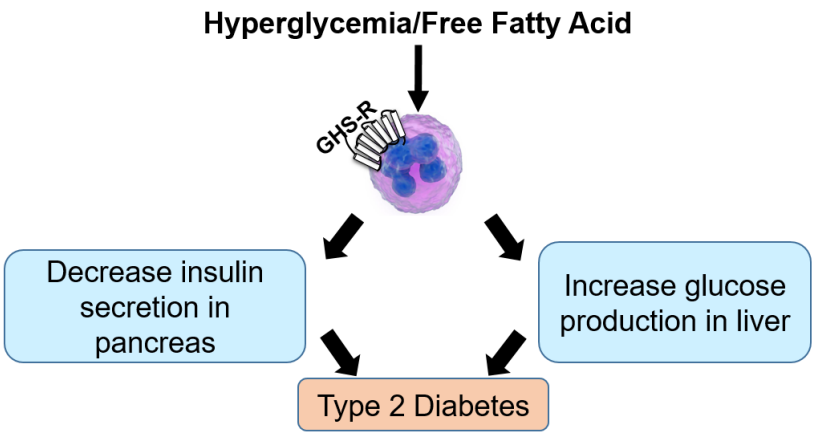

GHS-R in myeloid cells impairs insulin secretion and increases glucose production under T2D, possible due to the lack of IL-1Ra in islets

Figure 1. Hypothesis of myeloid-specific GHS-R mediated glucose dysregulation.

CHAPTER II

METHODS AND RESEARCH DESIGN

Mouse cohort

All mice handling and experiments are within IACUC guidelines **(2016-0292).** Experimental mice were generated by utilizing harem breeding requiring two females per male. Pure LysM-Cre males were bred with two $Ghsr^{f/f}$ females in single cages with access to ad libitum water and 9% fat diet. Age-matched, male LysM-Cre;$Ghsr^{f/f}$ and no cre;$Ghsr^{f/f}$ mice were chosen for the experiment and placed in cages of 4-5 with *ad libitum* access to water and regular diet from 4 weeks to 5-6 months. At 5-6 months of age, 11 LysM-Cre;$Ghsr^{f/f}$ and 12 $Ghsr^{f/f}$ male mice began high-fat diet feeding. We utilized HFD that has been shown to emulate metabolic syndrome better than others [77]. This formulation can be considered a "Western diet" due to high saturated fat content, high sucrose, .2% cholesterol content, and high total fat content (42%) **(Fig. 2)**. The classic Western diet is composed of high saturated fats and high sugar content and has been implicated in many chronic metabolic diseases. Western diet feeding and mice were terminated at 9-10 months old. Five to six-month old mice can be considered 'mature adults' and thus may serve as a reflective group to middle-aged men developing type 2 diabetes. Five to six-month mice were switched to Western diet feeding for 3 weeks before STZ injections and were kept on a western diet for the entirety of the experiment. Body weight and glucose were recorded weekly to bi-weekly, body composition and plasma were measured intermittently (8-9am).

Fig. 2	Western Diet	
	% by weight	% kcal from
Protein	17.3	15.2
Carbohydrate	48.5	42.7
Fat	21.2	42
Cholesterol	0.20%	-
	Ingredient	g/kg
	Casein	195
	DL-Methionine	3
	Sucrose	**341.46**
	Corn Starch	150
	Anhydrous Milkfat	210
	Cholesterol	**1.5**
	Cellulose	50
	Mineral Mix, AIN -76 (170915)	35
	Calcium Carbonate	4
	Vitamin Mix, Teklad (40060)	10
	Ethoxyquin	0.04

Figure 2. Composition of western diet. 42% of calories from fat, high in saturated fats, high in sucrose (34% by weight), and necessitates .2% total cholesterol. Formulation from Harlan Teklad (Madison, WI), TD.88.137.

Type 2 Diabetes induction

Briefly, the pathogenesis of T2D requires initial peripheral insulin resistance, followed by compensatory hyperinsulinemia, eventual beta-cell dysfunction, and an inability to regulate glycemia [1, 16, 23, 30, 41, 51, 58, 61, 84, 85]. Our induction method is based on similar protocols and has been repeatedly reported to best emulate a T2D state

in mice and rats [18-21]. Both groups of 5-6-month-old LysM-Cre; $Ghsr^{f/f}$ and $Ghsr^{f/f}$ mice were placed on a western diet, reported to induced metabolic syndrome, for 3 weeks to induce insulin resistance and hyperinsulinemia. Before western diet feeding, both groups had glucose measured, blood collected, and body weight/composition recorded; 1 and 3 weeks later this was repeated (**Fig. 3**). On day 22 (the day after week 3 data collection) mice began STZ (Sigma-Aldrich, St. Louis, MO) injections to induce beta-cell dysfunction. As mentioned earlier, the utilization of multiple low dose STZ (30-50mg/kg) injections are reported to be associated with macrophage or immune cell-mediated inflammation and injury of the beta-cell [22-24]. For this study we decided to use a 35mg/kg dose, based on previous experience, to administer. However, we later realized that this may have been insufficient and so we performed another set of STZ injections to further instigate a phenotype. In preparation, mice were fasted for 4 hours from 7 am to 11 am to allow for glucose to clear from blood but avoid increased endogenous glucose production from prolonged fasting. This is due to STZ and glucose competition for binding sites on beta-cell GLUT2 receptors [25]. STZ was weighed based on the most recent total body weight of the cohort, stored in Eppendorf tubes, and placed in -20C until needed. The solvent, Na-Citrate, was dissolved in 50ml of ddH20 at .1M and brought to a pH of 4.5 the day of injection, according to previous publications [11, 14, 16, 86]. Prior to injections, each reagent was placed on ice (in separate tubes) while the body weight of mice was calculated. STZ is photosensitive and degrades at a very rapid rate (15-20 minutes) once mixed with Na-Citrate buffer, so injections were carried out quickly. To avoid the chance of STZ degradation, several vials of STZ were prepared for 7-8 mice at

a time, as opposed to preparing one large mixture for all mice. Mice were anesthetized, according to IACUC guidelines, using isoflurane until breathing slowed and were unresponsive to footpad pinches. 35mg/kg dose was drawn up in 30g 1ml insulin syringe and injected intraperitoneally in the anesthetized mouse. Finally, mice were supplemented with 10% sucrose in drinking water to alleviate any symptoms of hypoglycemia characteristic of STZ exposure. These injections continued for 5 consecutive days total. Diabetic glucose levels were confirmed by consistent reading >250 mg/dl [26]. Mice were on western diet for the entirety of injections and up until termination.

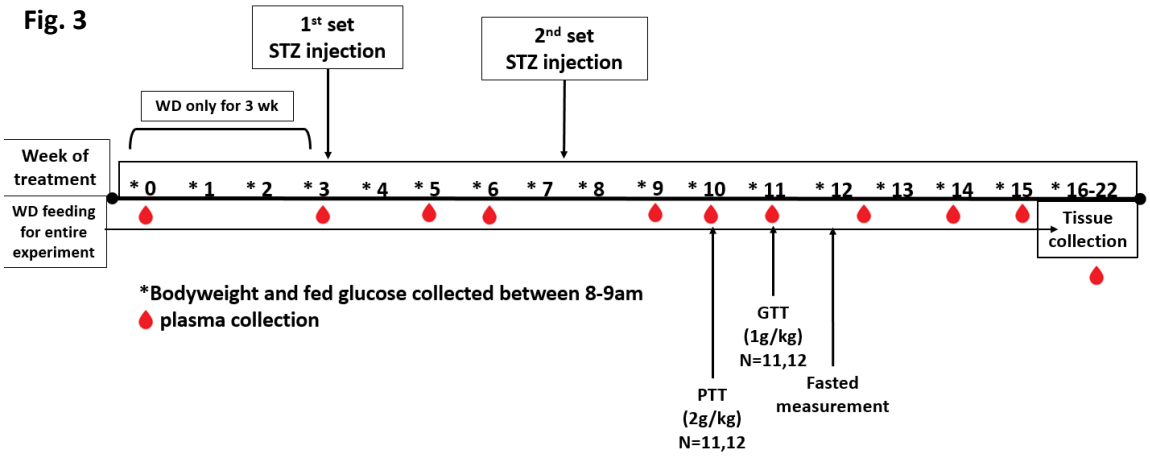

Figure 3. Timeline of T2D induction. Metabolic experiments, body weight and glucose measurement, and plasma collection. Western Diet feeding lasted for entire experiment.

RNA extraction, cDNA synthesis, and qPCR

Total RNA from islets was isolated using Arcturus PicoPure RNA Isolation Kit (Applied Biosystems, Vilnius, Lithuania), following the manufacturer's instructions. Total RNA from liver tissue was isolated using Aurum Total RNA Mini Kit (Bio-Rad, Hercules, CA), following the manufacturer's instructions. The cDNA was synthesized from 250-500ng RNA using the iScript Reverse Transcription Supermix for RT-qPCR (Bio-Rad, Hercules, CA). Real-time RT-PCR was performed on Bio-Rad Real-Time PCR Cycler (Bio-Rad Lab., Hercules, CA) using SYBR Green PCR Master Mix according to the protocol provided by the manufacturer. Relative gene expression levels were normalized by 18S rRNA. The primers were as follows GHS-R-1a: forward primer 5'-GGACCAGAACCACAAACAGACA-3', reverse primer 5'-CAGCAGAGGATGAAAGCAACA-3'[87], which can distinguish the functional receptor GHS-R1a from truncated receptor GHS-R1b. IL-1β: forward primer 5'-TGTTCTTTGAAGTTGACGGACCC-3', reverse primer 5'-TCATCTCGGAGCCTGTAGTGC-3'; IL-1R1: forward primer 5'-GCACGCCCAGGAGAATATGA-3', reverse primer 5'-AGAGGACACTTGCGAATATCAA-3'; IL-1RA: forward primer 5'-TTGTGCCAAGTCTGGAGATG-3', reverse primer 5'-TTCTCAGAGCGGATGAAGGT-3'. Glut2: forward primer 5'-ATCATTGGCACATCCTACT-3', reverse primer 5'-TCAGTTCCTCTTAGTCTCTTC-3'; IRS-1: forward primer 5'-GCCTGGAGTATTATGAGAACGAGAA-3', reverse primer 5'-

GGGGATCGAGCGTTTGG-3’; IRS-2: forward primer 5’-ACTTCCCAGGGTCCCACTGCTG-3’, reverse primer 5’-GGCTTTGGAGGTGCCACGATAG-3’; IGF-1: forward primer 5’-GGACCGAGGGGCTTTTACTT-3’, reverse primer 5’-CCGGAAGCAACACTCATCCA-3’; PDX-1: forward primer 5’-AGAGGGGGAACGACTCTAGG-3’, reverse primer 5’-ACTTGAGCGTTCCAATACGG-3’; Akt1: forward primer 5’-GACCCACGACCGCCTCTG-3’, reverse primer 5’-GACACAATCTCCGCACCATAGAAG -3’.

Pyruvate tolerance test (PTT)

Pyruvate tolerance test was performed on 11 LysM-cre;Ghsr $^{f/f}$ and 12 Ghsr$^{f/f}$ mice to record the differential response in hepatic glucose production. Similar to GTT, mice were fasted overnight for 16 hours (5 pm - 9 am), transferred to the procedure room, and placed in individual cages with *ad libitum* access to water. Na-Pyruvate dissolved in saline and filtered (.22µm), was made fresh the day of. 2g/kg doses were based on total body weight of mouse and were pre-measured before the start of the experiment. Tails were snipped using a small pair of scissors, glucose was measured using a OneTouch glucometer, and 50 µl of blood collected in 100 µl EDTA-coated tubes and placed on ice. 2g/kg Na-Pyruvate dose was then injected intraperitoneally (i.p.) using 1ml 30g insulin syringe. Timer started following the initial injection. Glucose was measured at 0, 15, 30, 60, and 120 minutes. Mice were then fed and placed in clean cages. Blood samples were then spun down and placed in -80C.

Glucose tolerance test (GTT)

Glucose tolerance test was performed on 11 LysM-cre;Ghsr $^{f/f}$ and 12 Ghsr$^{f/f}$ mice to record the differential response in glucose tolerance, as well as the insulin response. Mice were fasted overnight for 16 hours (5pm-9am) and transferred to the procedure room and placed in individual cages with *ad libitum* access to water. The glucose bolus was prepared the day of and dissolved in ddH20 and filtered (.22 µm) under a hood. 1g/kg doses based on total body weight of mouse were measured before start of experiment. After mice adjusted to transfer, tails were snipped using a small pair of scissors, glucose measured using a OneTouch glucometer, and 25 µl of blood was collected in 100ul EDTA-coated tubes and placed on ice. 1g/kg glucose dose was injected intraperitoneally (i.p.) using 1ml 30g insulin syringe. Timer started following initial injection. Glucose was measured at 0, 15, 30, 60, and 120 minutes and 25 µl of blood were at 0, 15, 30, and 60. Mice were then fed and placed in clean cages. Blood samples were then spun down and placed in -80C before using an ELISA kit (Mercodia, Uppsala, Sweden) to measure insulin.

Homeostatic model assessment of insulin resistance (HOMA-IR)

HOMA-IR was calculated based on fasting insulin and glucose levels from two different time points (weeks 11 and 12) and pooled together. The following HOMA-IR formula was used to calculate insulin resistance: HOMA-IR= fasting glucose (mmol/L)* fasting insulin (µU/L)/22.5 [80, 85]. Values above 2.9 were considered severely insulin resistant.

Tissue collection

The termination was in accordance with IACUC guidelines and all members involved were on the protocol (**2016-0292**). Tissue was collected from the cohort after 4-5 months from initial Western diet feeding. Two to three mice were sacrificed at a time to allow for ease of islet isolation and subsequent GSIS experiments the following day. Glucose and body weight were measured on the morning of (8:30am). Exposure to 2ml of isoflurane in a beaker was used to anesthetize mice and allowed for breathing to be slowed before confirming anesthetization with footpad pinches. Retro-orbital bleeding was utilized to collect .5 ml of blood for serum. Finally, mice were terminated using cervical dislocation. Pancreas was excised from mouse for islet isolation and body given to lab members for collection of other tissues. The liver, brain, WAT, BAT, and gastrocnemius were fixed in 10% formalin and transferred to 70% EtOH and stored in 4C the next day.

Islet isolation and culture

Following cervical dislocation, islets were collected using the collagenase method utilized by [27] and cultured overnight in low glucose RPMI media. Briefly, 3ml of .5-1mg/ml Collagenase P/BSA dissolved in ice-cold Hank's Balanced Salt Solution (HBSS) was injected via the pancreatic duct while the common bile duct near the liver was clamped. Once inflated, the pancreas was removed and placed in a 50 ml tube with 3 ml of Collagenase P solution. Tubes containing digest were then placed in 37 ^{o}C water bath at 100-120 shaking/min for 10-12 minutes. Subsequently, ice-cold 10% FBS solution + .2% BSA was added to digest tubes to stop collagenase P activity. The pancreatic digest

was then centrifuged using a Ficoll gradient Histopaque-1077 per manufacturer's instruction. Islets were then collected from the gradient, washed with more HBSS, handpicked using a 10 or 200 µl pipette under a dissection microscope at 12-16X magnification. Handpicking islets involved suspending islets in RPMI media and picking islets out of residual debris to be placed in fresh media. Subsequently, they were then incubated overnight, or placed in -80C, in RPMI-1640 medium containing 10% fetal bovine serum, 100 U/ml penicillin, 100 µg/ml streptomycin, 10 mM Hepes, 2 mM L-glutamine, 1 mM Sodium-pyruvate, 0.05 mM 2-mercaptoethanol and 5.5 mM glucose. The next day, the medium was replaced with Hanks' Balanced Salt Solution (HBSS) pH 7.2, consisting of 114 mM NaCl, 4.7 mM KCl, 1.2 mM KH^2PO^4, 1.16 mM $MgSO^4$, 20 mM HEPES, 2.5 mM $CaCl^2$, 25.5 mM $NaHCO^3$ 0.2% bovine serum albumin and 3.3 mM glucose for 2 hr. Following the 3.3 mM glucose incubation, islets were then incubated in either 3.3 mM or 22.2 mM glucose for another 2 hrs. HBSS buffer was then collected for insulin measurement using Mouse Insulin ELISA kit (Mercodia, Uppsala, Sweden) and normalized to islet protein content.

Glucose-stimulated insulin secretion (GSIS) assay

Once islets were collected from mice they were immediately placed in RPMI-1640 media supplemented with 10% fetal bovine serum, 100 U/mL penicillin, 100 µg/mL streptomycin, INS-1 cell supplement (10 mM Hepes, 2 mM L-glutamine, 1 mM Sodium-pyruvate, and 0.05 mM 2-mercaptoethanol), and 5.5Mm glucose. Then placed in a 37 C incubator overnight. The following day islets were removed from RPMI-1640 media using a 10 µl pipette and placed in HEPES Balanced Salt solution (HBSS) (114mM NaCl,

4.7mM KCl, 1.2mM KH2PO4, 1.16mM MgSO4, 20mM HEPES, 2.5mM CaCl2, 25.5 mM NaHCO3 and 0.2% bovine serum albumin, pH 7.2) supplemented with 3.3mM glucose for 2 hours. Fifteen minutes before the end of the 2 hours, two 12 well plates were prepared with 40 ul of HBSS w/3.3 mM glucose in each well. Once the 2-hour incubation in the low glucose-HBSS buffer was over, islets were divided into either a low (3.3 mM) or a high (22.2 mM) HBSS-glucose solution for another 2 hours. Briefly, 10 similarly sized islets/well were used for each condition. Low and high glucose conditions were assigned 4 and 6-8 replicates, respectively. For the purpose of our experiments, we were primarily interested in the GSIS response to high glucose solution, so this condition was prioritized. Once this was done each 12 well plate was placed in the 37C incubator for 2 hours; every 30 minutes they were shaken for 5 minutes on a plate shaker. After 2 hours, 200 µl of buffer solution was collected in PCR tubes and spun down for 3 minutes, 150 µl of supernatant was collected for insulin measurement and placed in -80C. The islets from each well were then collected using a 10 µl pipette, placed in Eppendorf tubes, stored in -80C, and later used to measure protein concentration for normalization to insulin secreted.

Islet protein, insulin/glucagon measurement, and relative secretion

Plasma insulin and glucagon were measured using the Mercodia Mouse Insulin or Glucagon ELISA kit (Mercodia, Uppsala, Sweden) and analyzed using cubic spline or 4 parameter fit analysis, respectively. Islet protein content was measured using linear regression analysis, represented as mg/ml using the Pierce™ BCA Protein Assay Kit (Thermo-Scientific, Illinois, United States). Insulin content from HBSS buffer was measured using cubic spline analysis, represented as ng/ml using Mercodia Ultra-

Sensitive Mouse Insulin Elisa kit (Mercodia, Uppsala, Sweden). Relative insulin secretion was calculated by dividing ng/ml of insulin by mg/ml of protein.

Cytokine multiplex

Serum samples from the time of tissue collection were used for analysis of cytokines (25 µl). Cytokines were measured using Milliplex MAP Mouse Cytokine/Chemokine (CAT# MECY2MAG-73KPX) according to manufacturers' instructions.

CHAPTER III

RESULTS

Body weight and body composition

Mice were 5-6 months old at the start of Western diet feeding (15%Pro, 42%CHO, 42%Fat). LysM-Cre;Ghsr$^{f/f}$ mice were on average larger than Ghsr$^{f/f}$ mice and remained so for the entirety of the experiment (**Fig. 4A**). However, when BW change ratio (BW(grams) of week X/ BW(grams) of week 0) was graphed we see no significant differences in BW ratio change (**Fig. 4B**). For both groups, we observe a rise in body weight followed by an expected drop due to STZ administration and then the maintenance of body weight. This is often reported in studies utilizing either low dose or high dose STZ treatment[14]. Weight loss is often observed in both insulin and non-insulin dependent diabetes and is primarily due to insulin deficiency. Additionally, comparing week 14 and week 0 both mice exhibited significantly increased fat mass even after STZ treatment. We see no differences in the fat ratio (**Fig. 4C**) or lean ratio change between the genotypes either. **Our results suggest that Western diet feeding induced equal significant increases of fat deposition for both groups, STZ administration induced weight loss due to insulin deficiency, and that fat mass was still significantly increased compared to week 0. In summary, both genotypes responded similarly to WD/STZ treatment.**

Fig. 4A

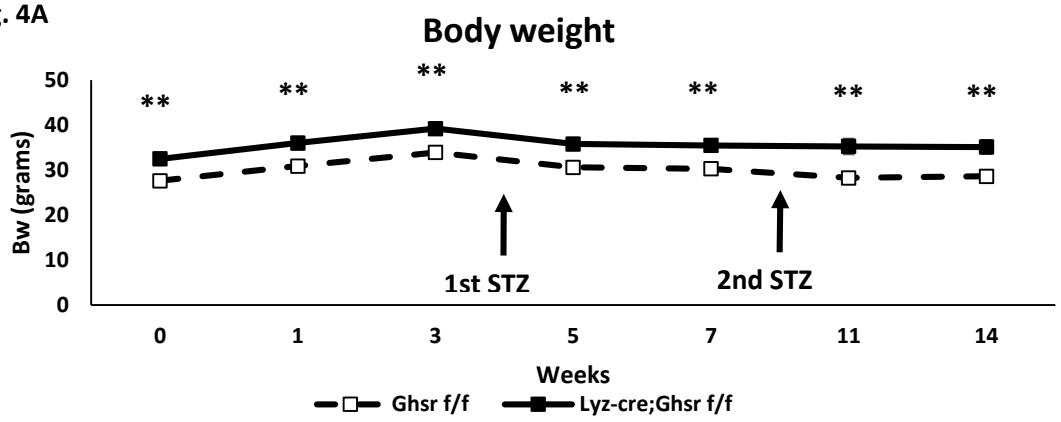

Fig. 4B

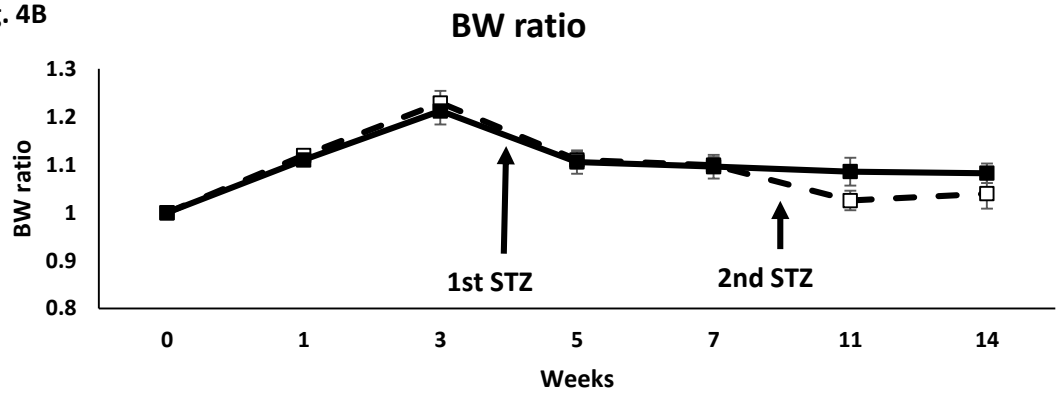

Fig. 4C

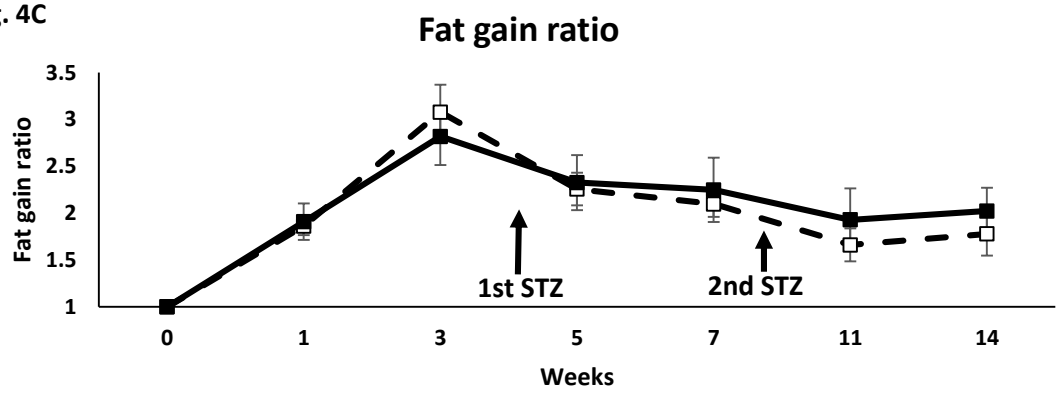

Figure 4. Body weight and ratio change. A) LysM-Cre;Ghsr$^{f/f}$ mice are larger throughout whole study. B) No difference in BW ratio gain between genotypes. C) No difference in fat ratio gain. * = p<.05, ** = p<.01, *** = p<.001 (between genotypes); N=11,12

Fed and fasted glucose

To assess the efficacy of WD/STZ treatment to induce hyperglycemia we measured glucose on a week to bi-weekly basis. Glucose was similar between both groups for the first 3 weeks of Western diet feeding (**Fig. 5A**). One week following STZ(5x35mg/kg) injections, glucose levels for both groups significantly increased, both groups reached glucose levels characteristic of T2D (>250mg/dl)[88, 89]. However, LysM-Cre;Ghsr$^{f/f}$ mice exhibited significantly lower glucose levels compared to Ghsr$^{f/f}$ ($p<.05$). The following two weeks (weeks 6-7) glucose levels did not appear to be significantly different. At this point we began another series of injections using the same dose of STZ, starting on week 7 and 8. On week 9 we measured glucose levels three times in a row and consistently observed significantly lower glucose levels in our LysM-Cre;Ghsr$^{f/f}$ mice. Later that week PTT (week 10) was performed followed by GTT (week 11) the next week. One week after GTT, we measured fasted glucose (week 12) and observed significantly lower glucose in LysM-Cre;Ghsr$^{f/f}$ mice. We observed fasted glucose (week 12) and fed glucose (week 13) were both significantly lower for LysM-Cre;Ghsr$^{f/f}$ compared Ghsr$^{f/f}$ (**Fig. 5B**). On week 14 we observed significantly lower glucose in LysM-Cre;Ghsr$^{f/f}$ mice, as well as glucose measured at the time of sac (weeks 16-22). **Our results suggest that in response to WD/STZ treatment LysM-Cre;Ghsr$^{f/f}$ mice exhibited attenuated hyperglycemia and lower fasting glucose levels.**

Fig. 5A

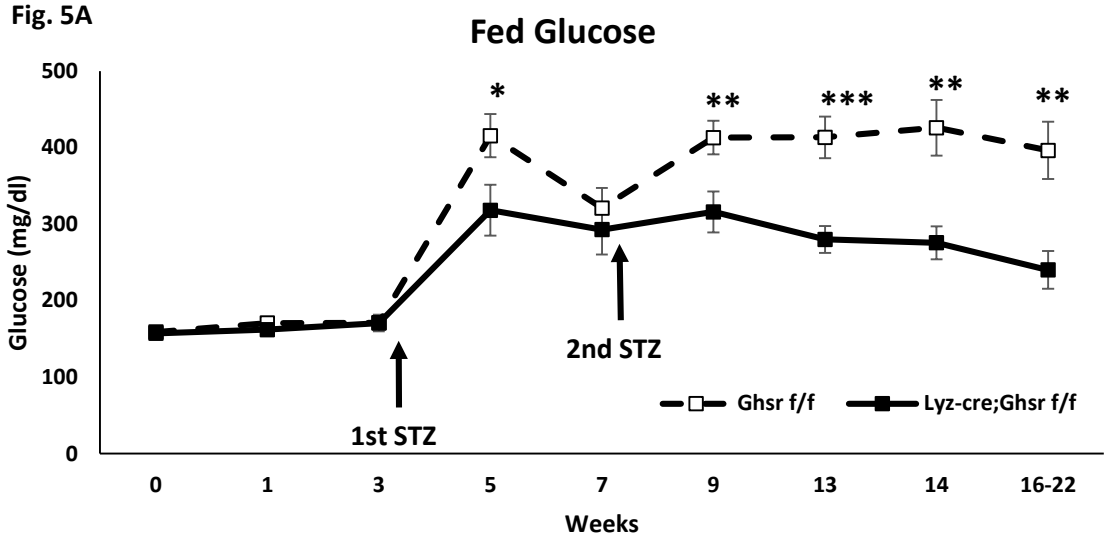

Fig. 5B

Figure 5. Fed and fasted glucose. A) In response to WD and STZ treatment, LysM-Cre; Ghsr$^{f/f}$ display attenuated fed glucose. B) LysM-Cre; Ghsr$^{f/f}$ exhibit significant reduction in both fed (wk. 13) and fasted (wk. 12) glucose compared to Ghsr$^{f/f}$ at late-stage of experiment. * = p<.05, ** = p<.01, *** = p<.001 (between genotypes); N=11,12

Fed and fasted insulin

To assess why LysM-Cre;Ghsr$^{f/f}$ mice displayed improved glucose levels we measured plasma concentration of insulin at key time points. At week 0 insulin was similar between both groups (**Fig. 6A**). At week 3, both groups exhibited significantly higher insulin levels compared to their respective week 0 concentrations. Additionally, we observed a trend for LysM-Cre;Ghsr$^{f/f}$ mice to have higher insulin levels. The unchanged glucose levels at week 0 and 3 is indicative of a hyperinsulinemic compensation for insulin resistance induced by WD feeding. Obesity, insulin resistance, and hyperinsulinemia are key characteristics of prediabetes and are so represented in this stage of our model[14]. On week 5, following STZ administration, insulin levels drop significantly for both groups compared to their respective week 0 concentration. This drop was expected and simulates the beta-cell dysfunction emblematic of T2D. Additionally, LysM-Cre;Ghsr$^{f/f}$ mice trended to have higher insulin ($p = .1$) compared to Ghsr$^{f/f}$ mice at week 5. On week 12, fasted insulin was significantly higher in LysM-Cre;Ghsr$^{f/f}$ mice compared to Ghsr$^{f/f}$ mice in conjunction with significantly lower glucose levels (**Fig. 6B**). Finally, LysM-Cre;Ghsr$^{f/f}$ mice exhibited significantly higher insulin compared to Ghsr$^{f/f}$ mice on week 13. **Our results suggest that in response to WD both groups compensate for insulin resistance via increased insulin production, STZ disrupted beta-cell compensation and resulted in hyperglycemia, and LysM-Cre;Ghsr$^{f/f}$ mice maintained higher insulin secretion under fed and fasted states, which was correlated with significantly lower glucose levels**

Fig. 6A

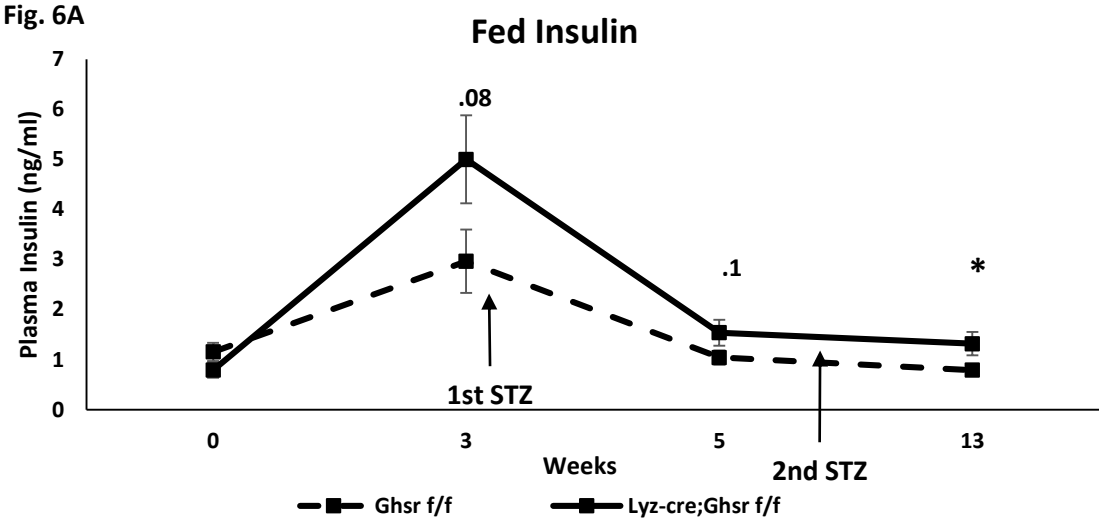

Fig. 6B

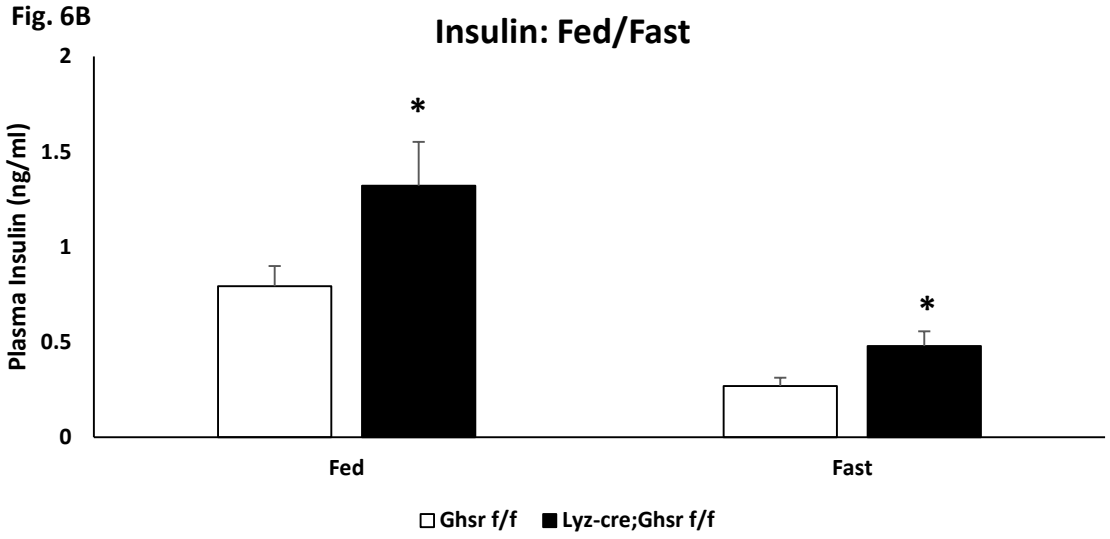

Figure 6. Fed and fasted insulin. A) In response to WD, LysM-Cre; Ghsr$^{f/f}$ display trend for higher circulating insulin compared to Ghsr$^{f/f}$. Following STZ, LysM-Cre; Ghsr$^{f/f}$ exhibits an initial trend for increased insulin, which then becomes significant as experiment progresses. B) LysM-Cre; Ghsr$^{f/f}$ exhibit significant increase in both fed (wk. 13) and fasted (wk. 12) insulin compared to Ghsr$^{f/f}$ at late-stage of experiment. * = p<.05, ** = p<.01, *** = p<.001 (between genotypes); N=11,12

Fed and fasted glucagon

Insulin downregulates glucagon expression and secretion from islet-resident alpha cells [90]. However, in the context of T2D, the insulin signaling pathway is disrupted as well as appropriate secretion of glucagon; this is characterized by hyperglucagonemia, increased HGP, and contributes to hyperglycemia. Similar to insulin we measured glucagon at several key time points (weeks 0, 3, 5, 12, and 13). At week 0, similar to insulin, we see no significant differences between plasma glucagon levels (**Fig. 7A**). Similar to insulin at week 3, we observe a significant rise in glucagon levels for both cohorts. This may be due to developing insulin resistance within the alpha cells, resulting in increased glucagon secretion. Additionally, proglucagon gene expression is reported to increase following HFD feeding [74]. On week 5, following STZ administration, we observed a drop in circulating glucagon, with no significant differences between genotypes. Glucagon secretion is reported to fall rapidly following STZ administration but increases over time [15]. Interestingly, on week 12 we measured fasted glucagon levels and found that they were lower than fed concentrations (**Fig. 7B**). We observed no differences between the genotypes. However, on week 13 we found that LysM-Cre;Ghsr$^{f/f}$ mice had significantly lower fed glucagon levels. Week 13 was also marked by significantly lower glucose and higher insulin concentrations. Our results suggest that WD/STZ treatment may have had a latent effect on circulating glucagon, which only exhibited itself after changes in insulin and glucose. **Overall, LysM-Cre;Ghsr$^{f/f}$ mice had lower circulating fed glucagon levels compared to Ghsr$^{f/f}$ in the later stages of the experiment.**

Fig. 7A

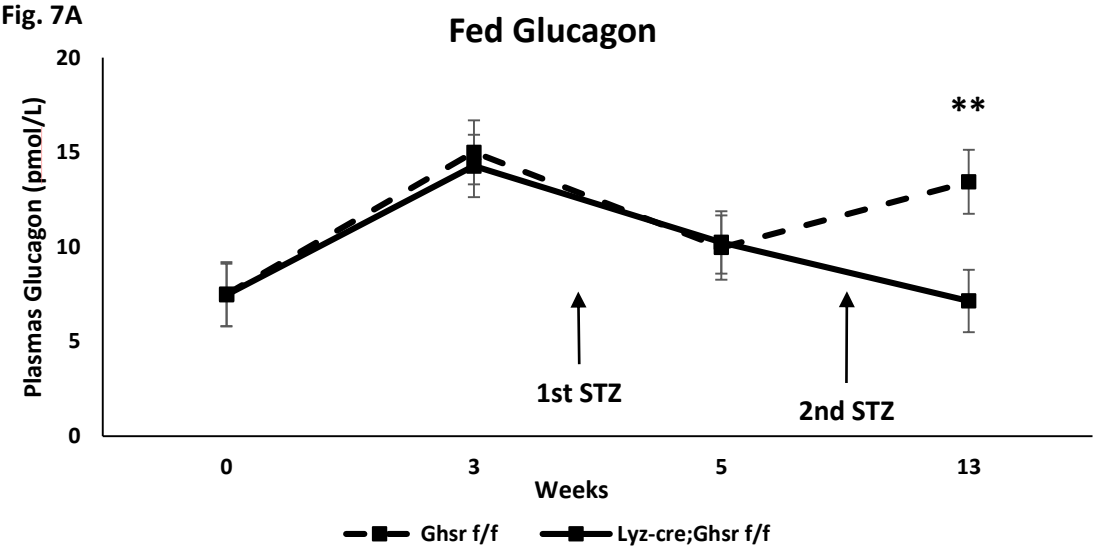

Fig. 7B

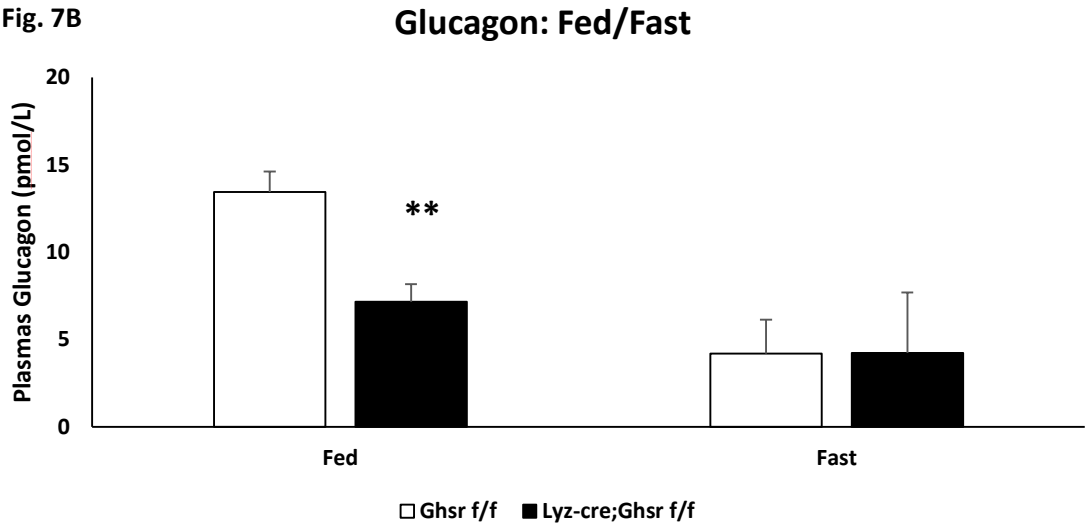

Figure 7. Fed and fasted glucagon. A) Week 0-5, LysM-Cre;Ghsr$^{f/f}$ and Ghsr$^{f/f}$ exhibit no differences, rise in response to WD, and fall following STZ. Week 13, LysM-Cre;Ghsr$^{f/f}$ have significantly lower glucagon compared to Ghsr$^{f/f}$. B) LysM-Cre; Ghsr$^{f/f}$ exhibit significant decrease in fed (wk. 13) but not fasted (wk. 12) glucagon compared to Ghsr$^{f/f}$ at late-stage of experiment. * = p<.05, ** = p<.01, *** = p<.001 (between genotypes); N=11,12

PTT

To assess hepatic glucose production in our diabetic mice we performed a pyruvate tolerance test on week 10. Pyruvate is used as a substrate in the gluconeogenic pathway and serves as a readout for the glucose producing activity of the liver. Under T2D, treatment often targets the suppression of HGP as it significantly contributes to hyperglycemia [91]. Fasting glucose levels were measured before administration of pyruvate dose. LysM-Cre;$Ghsr^{f/f}$ mice exhibited significantly lower glucose levels compared to $Ghsr^{f/f}$ at the zero time point (**Fig. 8A**). Glucose levels continued to be significantly lower throughout the entirety of the experiment (0-120 minutes). Additionally, when data was analyzed using the total area under the curve we find LysM-Cre; $Ghsr^{f/f}$ mice were exposed to a significantly lower amount of glucose ($p < .01$) (**Fig. 8B**). However, when we look at the percentage increase of glucose produced we observe either a trend or significantly higher rates of glucose produced in LysM-Cre;$Ghsr^{f/f}$ mice (**Fig. 8C**). Our results suggest that LysM-Cre;$Ghsr^{f/f}$ mice exhibit increased rates of glucose production but significantly lower total glucose exposure and production.

Fig. 8A

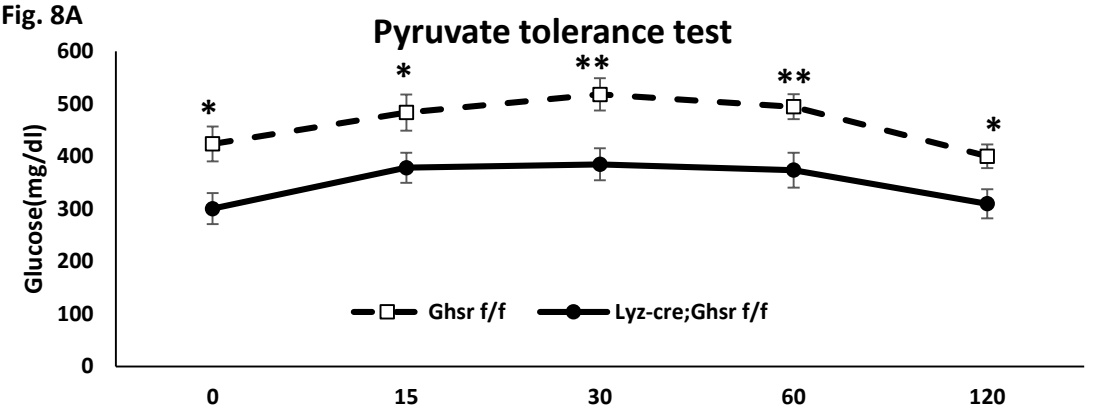

Fig. 8B

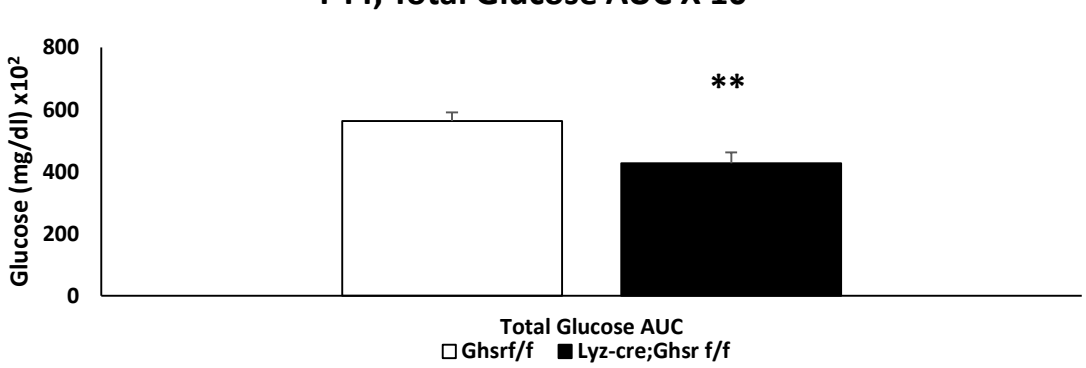

Fig. 8C

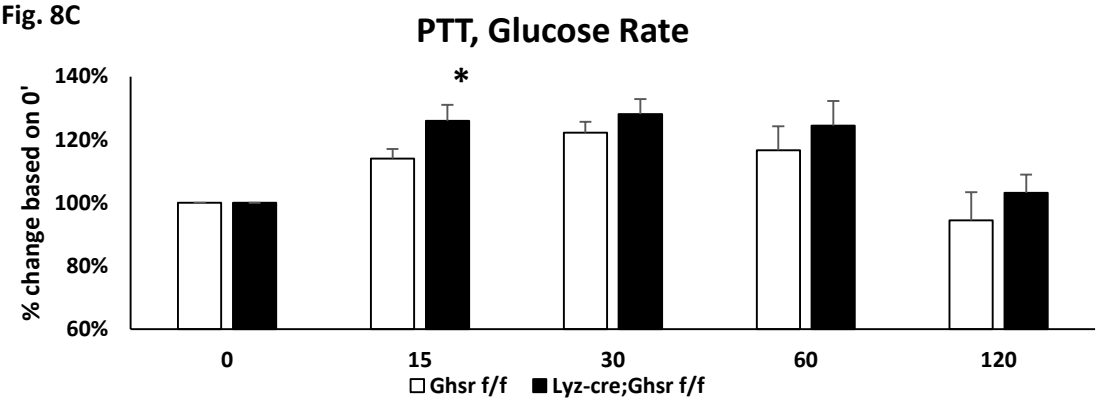

Figure 8. Pyruvate tolerance test. A) LysM-Cre;Ghsr f/f exhibited reduced glucose production, B) diminished total glucose exposure, and C) higher rate of glucose production at 15 minutes * = p<.05, ** = p<.01, *** = p<.001 (between genotypes); N=11,12 Performed on week 10

GTT

T2D is characterized by glucose intolerance and insulin secretion insufficiency. To assess the glucose handling ability of our diabetic mice we performed a glucose tolerance test on wk 11. Glucose was measured in 16 hr fasted mice after acclimatization to room transfer. Similar to PTT, we observed significantly lower glucose levels at the zero-time point in LysM-Cre;Ghsr$^{f/f}$ mice. LysM-Cre;Ghsr$^{f/f}$ mice continued to exhibit significantly lower glucose levels for the remaining time points (**Fig. 9A**). We collected plasma at 0, 15, 30, and 60 minutes to measure the insulin response. Insulin concentrations were identical at the zero-time point (**Fig. 9B**). At 30 and 60 minutes, Ghsr$^{f/f}$ insulin concentrations did not rise/respond to glucose administration. LysM-Cre; Ghsr$^{f/f}$ mice exhibited trends for increased insulin concentrations but this was not significantly higher compared to Ghsr$^{f/f}$ mice. Interestingly, at 60 minutes Ghsr$^{f/f}$ insulin trended to be lower than at 0 minutes (p=.21). Comparing both LysM-Cre;Ghsr$^{f/f}$ and Ghsr$^{f/f}$ mice at 60 minutes, we observed that LysM-Cre;Ghsr$^{f/f}$ mice had significantly higher levels of insulin, while Ghsr$^{f/f}$ mice trended to be lower than its own zero-time point. Additionally, when the data was analyzed using total area under the curve we find that LysM-Cre;Ghsr$^{f/f}$ mice were exposed to significantly lower glucose (**Fig. 9C**). At 15 minutes we find that LysM-Cre;Ghsr$^{f/f}$ mice exhibited a significant 90% increase in glucose levels compared to the 60% increase in Ghsr$^{f/f}$ mice (**Fig. 9D**). However, this significant difference did not continue for the rest of the experiment. **Our results suggest that LysM-Cre;Ghsr$^{f/f}$ mice have lower fasting glucose levels, improved glucose tolerance, and improve insulin response to rising glucose levels.**

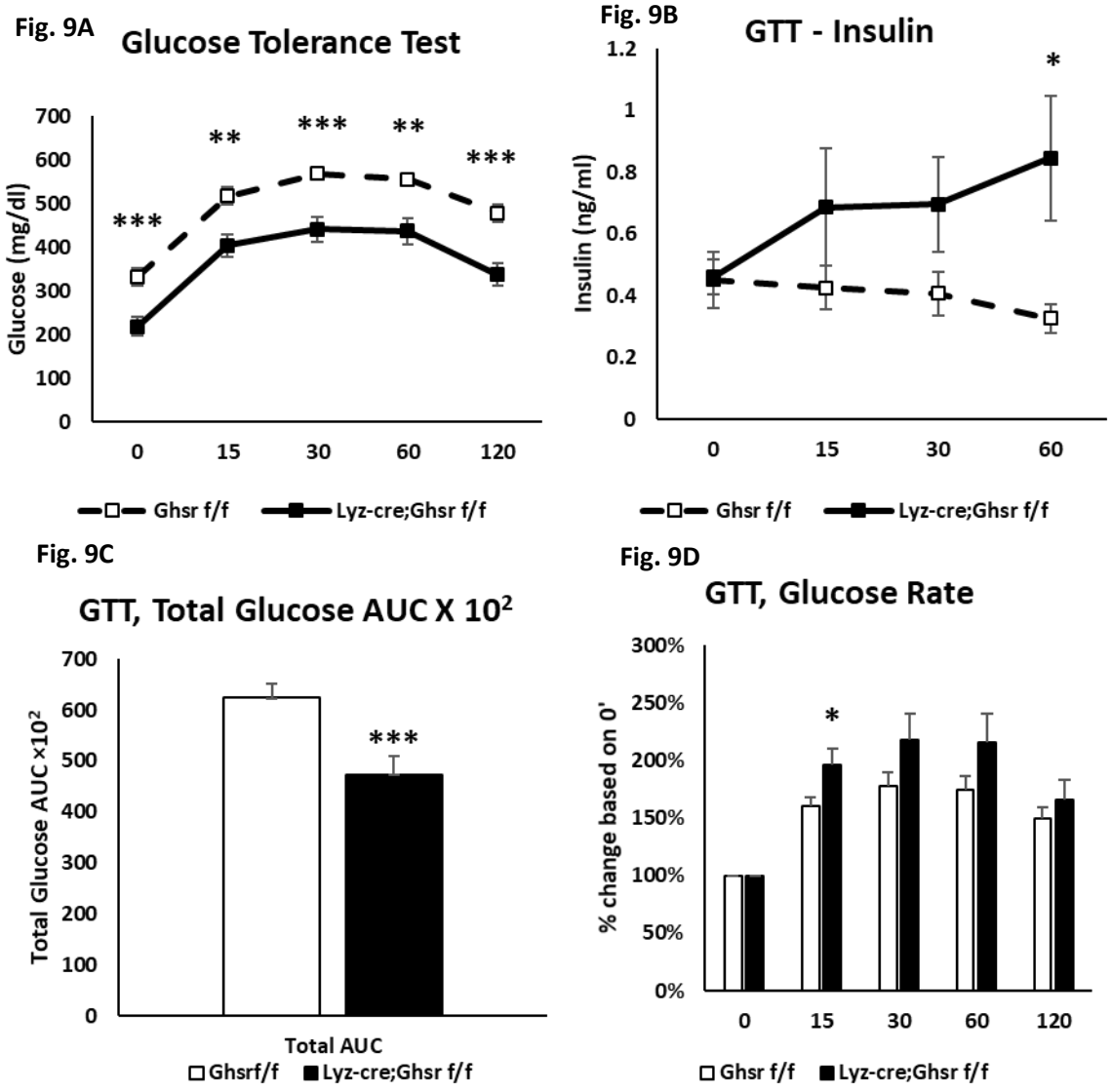

Figure 9. Glucose tolerance test. A) LysM-Cre;Ghsr$^{f/f}$ mice exhibited improved glucose tolerance, B) increased insulin response, C) diminished total glucose exposure and D) increase rate of glucose at 15 minutes. Performed on week 11
*** = p<.05, ** = p<.01, *** = p<.001 (between genotypes); N=11,12**

HOMA-IR

To determine whether differences in glucose tolerance and hepatic glucose production were due to variations of insulin sensitivity, we calculated HOMA-IR. Data points were pooled from fasted glucose/plasma from week 12 and GTT (week 11). The physiological basis of HOMA-IR is to determine an estimate of beta-cell function and insulin sensitivity from fasting insulin and glucose [92]. The balance between insulin secretion and HGP is reflected by the relationship between glucose and insulin during fasted or basal conditions. The following HOMA-IR formula was used to calculate insulin resistance: HOMA-IR= fasting glucose (mmol/L)* fasting insulin (μU/L)/22.5 [84, 93]. Values above 2.9 were considered severely insulin resistant [94]. Both mice exhibited HOMA-IR index scores that were insulin resistant and there were no significant differences between the two genotypes (**Fig. 10**). These results suggest that both cohorts of mice were profoundly insulin resistant as a result of WD feeding.

Fig. 10

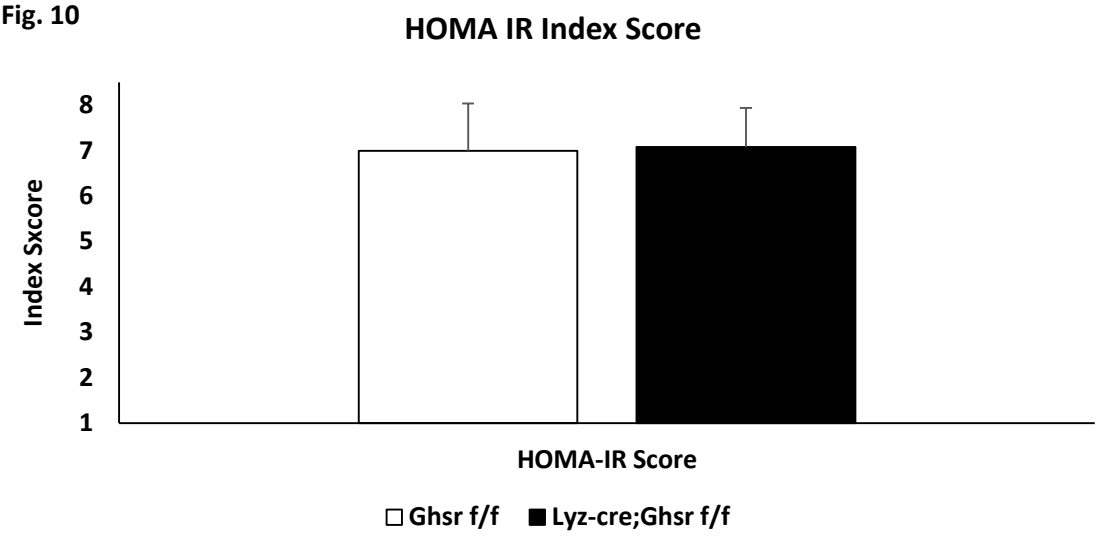

Figure 10. HOMA-IR. Both genotypes exhibited scores indicative of insulin resistance. ***HOMA-IR= fasting glucose (mmol/L)* fasting insulin (µU/L)/22.5;*** **N= 11,12**

Ex vivo GSIS

To assess the impact of T2D induction on the insulin secretory capacity of islets, we exposed islets to either low or high concentration of glucose in HBSS buffer. More specifically, we were interested in the impact that myeloid-specific GHS-R inhibition had on pancreatic islet function. When $Ghsr^{f/f}$ islets were exposed to either 3.3mM or 22.2mM glucose concentrations we observed no difference between low or high concentrations (**Fig. 11**). Interestingly, elevated basal insulin secretion is a hallmark of beta-cell dysfunction in T2D [30, 95]. However, when LysM-Cre;$Ghsr^{f/f}$ islets were exposed to either 3.3mM or 22.2mM glucose concentrations we observed significantly higher insulin secretion at 22.2mM compared to 3.3mM. Interestingly, when we compared islets of both

genotypes at low glucose condition we observe significantly lower insulin secreted in LysM-Cre;Ghsr$^{f/f}$ islets. We see no difference in insulin secretion at high glucose concentration when comparing both genotypes. Our results suggest that islets from LysM-Cre;Ghsr$^{f/f}$ mice exhibit an improved ability to regulate both basal and stimulatory insulin secretion compared to Ghsr$^{f/f}$ mice.

Fig. 11

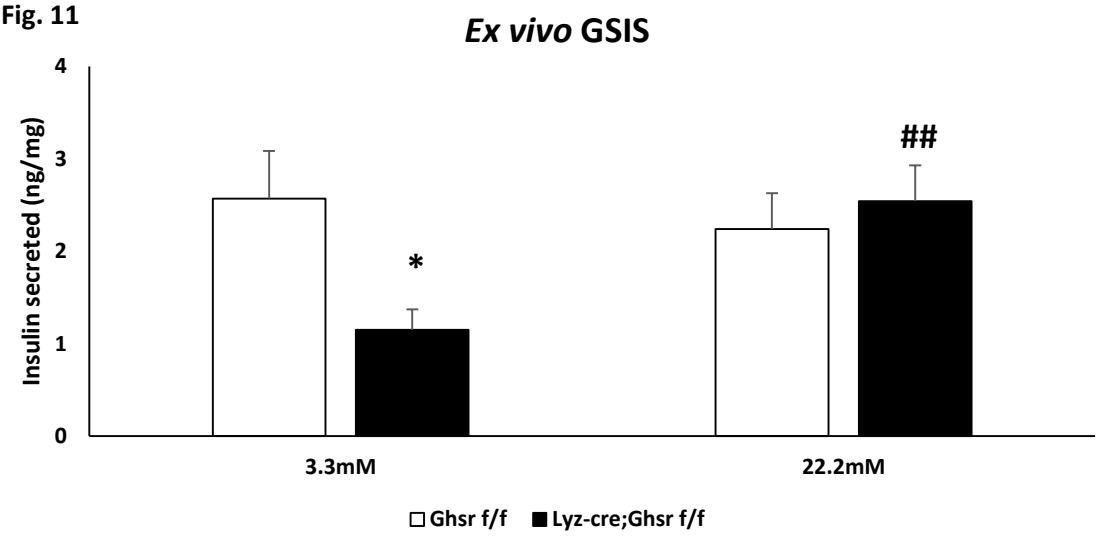

Figure 11. LysM-Cre;Ghsr$^{f/f}$ islets exhibit improved GSIS regulation. LysM-Cre;Ghsr$^{f/f}$ secreted significantly lower insulin at basal conditions compared to Ghsr$^{f/f}$. Under stimulatory conditions LysM-Cre;Ghsr$^{f/f}$ secretes significantly more insulin compared to basal conditions. No difference in insulin secreted between basal and stimulatory conditions for Ghsr$^{f/f}$. * = p<.05, ** = p<.01, *** = p<.001 (between genotypes); # = p<.05, ## = p<.01, ### = p<.001 (between conditions); N=5,6 (mice)

Islet gene expression

Inflammatory signaling has been reported to impact GSIS and insulin signaling to induce beta-cell dysfunction and T2D [1, 23, 29, 96]. To investigate changes in insulin signaling and GSIS-related genes we measured IGF-1, IRS1, IRS2, AKT1, PDX1, and GLUT2 from whole islet tissue (**Fig. 12A**). We observed a significant increase in all genes from LysM-Cre;Ghsrf/f whole islet tissue. IGF-1 is reported to promote beta-cell proliferation, inhibit cell death, and maintain insulin secretion in spite of beta-cell death[97, 98]. IRS-2 is necessary for beta-cell compensation of insulin resistance and its deficiency leads to overt diabetes[99], while IRS-1 deficiency impairs beta-cell GSIS response to glucose[100]. Reduction in AKT1 signaling is reported to induce insulin resistance in beta-cells and functionality, as it further regulates expression of PDX1 and GLUT2 [96]. PDX1 expression increases in response to hyperglycemic conditions and is correlated to increased beta-cell replication and survival; its expression decreases under T2D[49]. Similarly, GLUT2 deficiency is observed in diabetic rodent models and is characterized as attenuated GSIS via impaired glucose sensing [101]. Overall, LysM-Cre;Ghsr$^{f/f}$ exhibited increased expression of key insulin signaling genes related to GSIS and glucose sensing.

Additionally, we investigated changes in IL-1R1, IL-1Ra, and IL-1β. (**Fig. 12B**). We observed a significant increase in IL-1R1 and IL-1Ra expression in LysM-Cre;Ghsr$^{f/f}$ islet tissue. IL-1R1 is reported to be 10 fold higher in isolated islet than in pancreas and within islets is higher in beta-cells than alpha cells[56]. The significant increase of IL-1R1 we observed may be an indirect measure of beta-cell population. Additionally, we

observed a trend for increased IL-1β expression. However, the increase in IL-1β was paralleled by the significant increase of IL-1Ra, which has been associated with inhibition of IL-1β activity and improvement of T2D symptoms [3, 42, 57, 58, 60]. Furthermore, we've postulated that LysM-Cre;Ghsr$^{f/f}$ mice may promote a re-balancing of the IL-1Ra: IL-1-β ratio to levels similar to the compensatory period prior to the onset of T2D. The increased IL-1Ra we see may be counteracting IL-1β induced signaling of IL-1R1 and downstream activation of other inflammatory mechanisms. **Overall, we report a significant increase in the expression of key insulin signaling genes related to proper beta-cell functionality and improvements in the expression of IL-1Ra: IL-1β.**

Fig. 12A

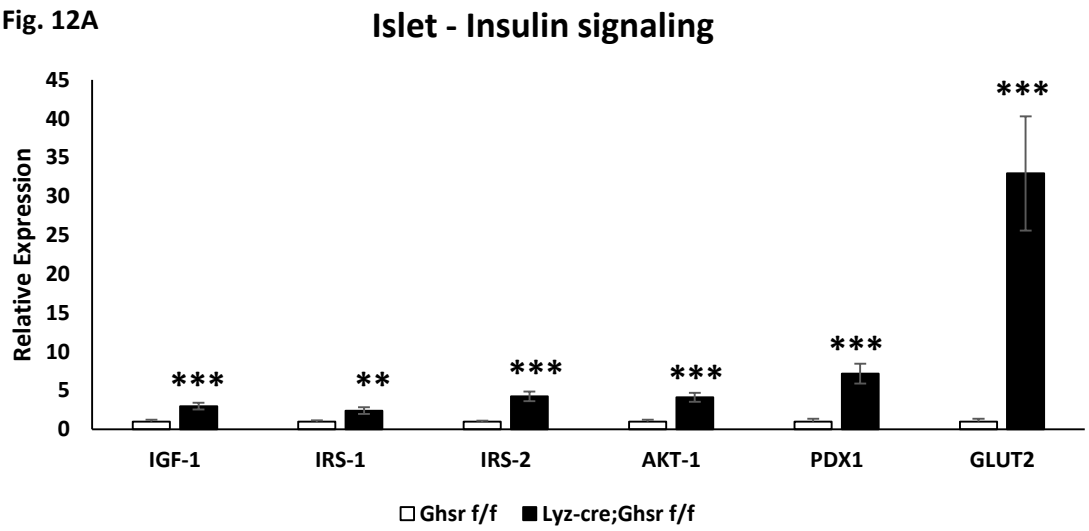

Fig. 12B

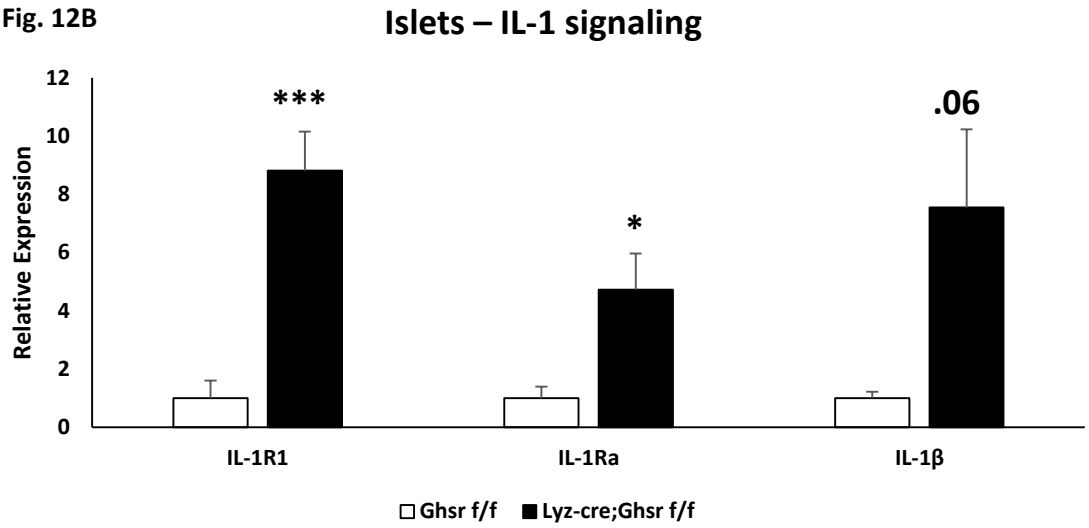

Figure 12. Islet gene expression. Significant increased expression of all insulin signaling genes, IL-1R1, and IL-1Ra in LysM-Cre;Ghsr$^{f/f}$ islet tissue. Other insulin signaling genes exhibit increased trend in LysM-Cre; Ghsr$^{f/f}$ islet tissue. * = p<.05, ** = p<.01, *** = p<.001 (between genotypes); N=5,6 (mice)

Cytokine multiplex

To investigate systemic inflammation differences between genotypes we ran samples from the time of tissue collection on a multiplex kit. We observed reduced trends for IL-1β, IL-6, and TNF-α in LysM-Cre;Ghsr$^{f/f}$ (**Fig. 13**). HFD-mediated inflammation has been associated with the increased systemic circulation of IL-1β, IL-6, and TNF-α[102]. While none reach statistical significance, we believe that this is biologically significant. The concomitant reduction of IL-1β, IL-6, TNF-α suggests an improvement of the systematic inflammatory milieu. TNF-α has been associated with worsening insulin resistance and contributes to the pathogenesis of T2D [103], IL-6 is reported to inhibit GSIS and impair insulin sensitivity in the liver[104], and pancreatic beta-cells are highly sensitivity to IL-1β as they very highly express the IL-1R1 receptor[56]. **In summary, LysM-Cre;Ghsr$^{f/f}$ exhibited a trend for reduction in circulating inflammatory proteins**

Fig. 13

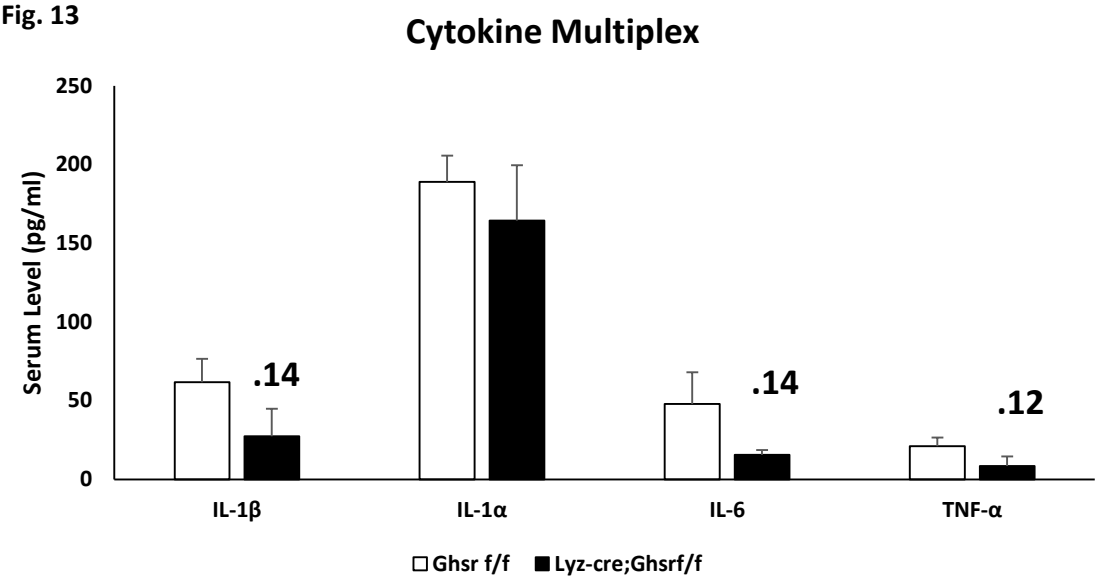

Figure 13. Cytokine multiplex. LysM-Cre;Ghsr f/f serum samples exhibited trend for decreased inflammatory cytokines : IL-1β, IL-6, TNF-α. ***A collaborative effort with Da Mi Kim***

CHAPTER IV

DISCUSSION

In this study, the effect of myeloid-specific GHS-R was observed under simulated type 2 diabetic conditions utilizing the WD + multiple low dose streptozotocin method. We took note of changes in glucose homeostasis, glucoregulatory hormones, metabolic tests, as well as changes in gene expression and serum cytokines to characterize differences between LysM-Cre;$Ghsr^{f/f}$ and $Ghsr^{f/f}$. The result of this was the finding that inhibition of myeloid-specific GHS-R attenuates the severity of T2D symptoms possibly via improvements in systemic inflammation and islet-related IL-1Ra: IL-1β homeostasis.

The utilization of the WD/STZ model was successful in emulating the natural pathogenesis and metabolic profile of T2D. This was confirmed by WD-induced insulin resistance followed by compensatory hyperinsulinemia (**Fig. 6A**) in conjunction with the maintenance of euglycemia (**Fig. 5A**). Subsequently, STZ administration induced insulin deficiency, similar to the starting point, (**Fig. 6A**) in parallel with hyperglycemia (**Fig. 5A**). Similar to other studies using this method, our model emulated late-stage T2D, due to hyperglycemia and insulin levels similar to pre-HFD feeding[14, 73]. Glucagon levels were significantly higher at week 13 for $Ghsr^{f/f}$ suggesting increased activity of alpha cells to secrete glucagon, commonly seen in T2D (**Fig. 7A**) [105]. Hyperglycemia was confirmed as readings of fed glucose >250 mg/dl[29]. Both LysM-Cre;$Ghsr^{f/f}$ and $Ghsr^{f/f}$ responded similarly to WD/STZ but LysM-Cre;$Ghsr^{f/f}$ exhibited attenuated symptoms compared to $Ghsr^{f/f}$ mice.

Previous studies utilizing the HFD + multiple low dose STZ have reported similar characteristics in their findings. *Nath et al*. developed a similar regimen where both male and female, 6-8 week old Swiss albino mice were fed HFD (58%) for 3 weeks followed by 5 consecutive doses of 40mg/kg streptozotocin [11]. HFD feeding ended after the last STZ injection, mice were then placed on the regular chow diet and allowed 1 week for hyperglycemia to stabilize. They concluded that the HFD + low dose STZ emulated the metabolic characteristics of T2D via analysis of histological change in key tissues, glucose metabolism, lipid profiles, and anti-oxidant activity. *Srinivasan et al* performed a similar study using different doses of STZ (25-55mg/kg), normal chow-fed, and HFD-fed (58%) Sprague-Dawley rats (age not mentioned)[106]. HFD feeding induced obesity, mild hyperglycemia, hypertriglyceridemia, hypercholesterolemia and compensatory hyperinsulinemia, a condition similar to prediabetes. After 2 weeks of either HFD or regular chow, groups of rats were injected with varying doses of STZ. STZ doses of 45-55mg/kg induced significant hyperglycemia, insulin deficiency, significant weight loss, and death in some cases for both normal and HFD fed mice. The 35 mg/kg dose induced hyperglycemia only in HFD-group and reduced insulin to levels similar to the regular-chow group; emulating the pathophysiology of non-insulin dependent diabetes.

Our model differed from these studies in several ways including use of 5-6-month-old mice, C57BL/6 mice, use of prolonged WD feeding, a lower dose of STZ, measurement of fed glucose instead of fasted, and longer duration of the experiment. Furthermore, our model measured circulating insulin/glucagon at key time points allowing greater insight of the changes in glucoregulatory hormones. The choice of older male mice

allowed us to better understand the similar effect that would be seen in mature adults as opposed to T2D pathogenesis in young adults. Additionally, most studies using this model tend to include rodents < 6 months old[14]; our study utilized 5-6-month-old mice and followed their metabolic profile until they were 9-10 months old. Also the choice to continue WD also better emulates the reality of human diabetics continuing consumption of an unhealthy diet following the diagnosis of T2D. Additionally, compared to other HFD and VHFD, the use of our Western diet is reported to better induce metabolic syndrome, a major risk factor for the development of T2D [77]. The need for a 2nd set of STZ doses to fully characterize our phenotype also suggests some resistance that C57BL/6 mice have compared to the Sprague-Dawley rats. While there were certainly differences in various parameters, ours and others still followed a regimen of HFD-induced insulin resistance/hyperinsulinemia for several weeks followed by multiple low doses of STZ to instill insulin deficiency and subsequent hyperglycemia.

To our knowledge, the use of prolonged Western diet in combination with low dose STZ in our study is the first of its kind. We believe that the use of WD and low dose STZ exhibits the metabolic profile of late-stage diabetes and that myeloid-specific inhibition of GHS-R attenuated the severity of T2D. While the use of this model has yet to be proven to induce the same inflammatory/oxidative milieu seen within islet tissue during naturally occurring T2D, it has been shown to simulate the metabolic profile of T2D [11, 74]. However, several have reported that low dose administration of STZ induces a gradual loss of beta-cell function mediated by immune cells, including macrophages and cytokines[13, 18, 19, 74, 75]. HFD feeding has been shown to induce insulin resistance

and chronic low-grade inflammation. The use of western diet formulas has been reported to more effectively instill metabolic syndrome within mice compared to even VHFD[77]. Metabolic syndrome is a prime risk factor for the occurrence of T2D[107, 108], thus our utilization of WD to prime our mice before STZ treatment may be an improvement on the standard HFD/VHFD regimen. Our combination of western diet (known to instill metabolic syndrome and low grade inflammation) and low dose streptozotocin (known to reduce beta-cell function via immune-related mechanisms) may best exemplify a type 2 diabetic state in a relatively short time frame. Furthermore, long-lasting hyperglycemia amid western diet feeding, multiple weeks/months following WD/STZ treatment may better reflect the T2D state than at its initial induction 1-2 weeks post-treatment. In short, multiple weeks or months following WD/STZ treatment may better reflect the T2D state than 1-2 weeks following T2D induction, which we were able to observe in our study. The use of the HFD/STZ treatment provides researchers with a quick and dirty platform to establish a proof-of-concept study. In our case, we observed that under simulated T2D conditions, myeloid-specific inhibition of GHS-R attenuated the severity of T2D symptoms.

Based on the attenuated hyperglycemia, glucagon, and improved circulating insulin in LysM-Cre;Ghsr$^{f/f}$ mice we further investigated changes in metabolic regulation of glucose production and tolerance. Glucose and pyruvate tolerance tests further supported our findings, revealing significantly lower total glucose exposure in both tests (**Fig. 8B, 9C**) and improved insulin response during GTT (**Fig. 9B**). Comparing the insulin response between LysM-Cre;Ghsr$^{f/f}$ and Ghsr$^{f/f}$ mice suggests that Ghsr$^{f/f}$ have a

diminished first phase insulin response, often described as "earliest detectable defect of β-cell function" [109]. Under T2D, treatment often targets suppression of HGP as it significantly contributes to hyperglycemia [91]. Uncontrolled hyperglycemia in conjunction with insulin resistance and insulin deficiency is a leading cause of diabetes-related complications in multiples tissues, thus strategies reducing total glucose exposure are imperative[110]. Taken together with the reduction in total glucose exposure and improved first phase insulin response observed from both these tests suggest that inhibition of myeloid-specific GHS-R may serve as a therapeutic target.

T2D is associated with the increased production of IL-1β which signals via IL-1R1 to activate downstream target NF-κB and JNK [111]. HFD/STZ treatment has been reported to increase expression and protein levels of TNF-α, IL-6, and IL-1β [74]. NF-κB and JNK attenuate the activity of IRS-1 and subsequently activation of AKT. The interruption of these key insulin signaling genes prevents proper GSIS functioning and survival of pancreatic beta-cells [48, 50]. To determine whether WD/STZ treatment diminished beta-cell function we performed *ex vivo* GSIS and analyzed the gene profile of whole islet tissue. We found that LysM-Cre;$Ghsr^{f/f}$ mice exhibit an improved ability to regulate both basal and stimulatory insulin secretion compared to $Ghsr^{f/f}$ mice, suggesting improved glucose sensing (**Fig. 11**). Upon analysis of whole islet tissue from each group, we observed significant increases of insulin signaling genes from LysM-Cre;$Ghsr^{f/f}$. This included significant increases of IGF-1, IRS-1, IRS-2, and AKT-1 (**Fig. 12A**); a deficiency in any of these is reported to impede beta-cell function and survival [98-100]. The significantly increased expression of GLUT2 and PDX1 from LysM-Cre;$Ghsr^{f/f}$ mice

supports the notion of improved glucose sensing in our *ex vivo* GSIS data. PDX1 and GLUT2 deficiency is observed in diabetic rodent models and is characterized as attenuated GSIS via impaired glucose sensing[101]. The improved expression of insulin signaling and GSIS-related genes may be in part due to improvements in IL-1 expression.

Pre-clinical and clinical trials have reported that IL-1Ra improved glucose homeostasis, insulin secretion, and reduced systemic inflammation [57]. This effect lasted well beyond end of treatment and may be attributed to the interruption of an IL-1β feed-back loop between macrophages and beta-cells [58]. Some have postulated that interruption of IL-1β activity may allow for a rebalancing of the IL-1Ra: IL-1β homeostasis and aide in attenuating severity of diabetes and inflammatory disorders[60]. Similarly, other studies have reported that low-dose streptozotocin induced hyperglycemia was prevented by the continuous administration of IL-1Ra, suggesting a key role for IL-1Ra in attenuating the severity of STZ-induced diabetes [112]. We found significantly increased expression for both IL-1Ra and IL-1R1, but only a trend for increased IL-1β (**Fig. 12B**).

Furthermore, IL-1Ra is reported to predominantly originate from beta-cells [5]. The parallel significant increase in IL-1R1, IL-1Ra, and PDX1 suggest not only improved beta-cell function but also an indirect measure of the number of beta-cells in islet tissue. PDX1 is a beta-cell-specific gene and has a key role in maintaining beta-cell identity and preventing de-differentiation into alpha cells[51], IL-1Ra is predominantly expressed in the beta-cells[5], and IL-1R1 is most highly expressed in beta-cells[56]; taken together this suggests that myeloid-specific inhibition of GHS-R improved beta-cell functionality

and possibly number of beta-cells in whole islet tissue. IL-1β signaling is reported to activated NF-κB and JNK activity[42], which are known to inhibit insulin signaling and induced beta-cell death. While we did not measure NF-κB or JNK protein we did find evidence that their activity was blunted via the improvements of key insulin signaling genes in whole islet tissue. Further investigation into these proteins is warranted. IL-1β also did not reach statistically significant levels of expression and the phenotype that chronic IL-1β induces was also not observed in LysM-Cre;Ghsr$^{f/f}$. In summary, myeloid-specific inhibition of GHS-R may have re-established the IL-1Ra: IL-1β ratio, which was correlated with increased insulin signaling genes, suggesting increased IL-1Ra activity based on improvements seen in phenotype.

HFD-mediated inflammation has been associated with increased systemic circulation of IL-1β, IL-6, and TNF-α[102]. Multiplex analysis of serum cytokines revealed a trend for a reduction in several key inflammatory cytokines in LysM-Cre;Ghsr$^{f/f}$. While none reach statistical significance, we believe that this is biologically significant. The concomitant reduction of IL-1β, IL-6, TNF-α suggest an improvement of the systematic inflammatory milieu. TNF-α has been associated with worsening insulin resistance and contributes to the pathogenesis of T2D[103], IL-6 is reported to inhibit GSIS and impair insulin sensitivity in liver[104], and pancreatic beta-cells are highly sensitivity to IL-1β as they very highly express the IL-1R1 receptor[56]. We have previously reported that global GHS-R knockout in response to HFCS feeding exhibited attenuated adipose tissue concentration of TNF-a, IL-6, and IL-1β[7]. In summary, LysM-

Cre;Ghsr$^{f/f}$ exhibited a trend for reduction in circulating inflammatory proteins.

CHAPTER V

CONCLUSIONS AND FUTURE DIRECTIONS

In conclusion, this study investigated the impact myeloid-specific inhibition of GHS-R had in response to T2D induction using the WD + multiple low dose method. The WD/STZ method simulated the natural progression of T2D, the severity of which was attenuated in LysM-Cre;Ghsr$^{f/f}$. This reduction is severity was confirmed by attenuated hyperglycemia (**Fig. 5A**), increased insulin (**Fig. 6A**), lower glucagon (**Fig. 7A**), improved hepatic glucose production (**Fig. 8A**), improved glucose tolerance (**Fig. 9A**), and enhanced insulin secretion *in vivo* (**Fig. 9B**) and *ex vivo* (**Fig. 11**). Furthermore, gene expression of whole islet tissue exhibited increased insulin signaling genes (**Fig. 12A**) and improvement of IL-1Ra: IL-1β (**Fig. 12B**), suggesting increased IL-1Ra activity. Myeloid-specific inhibition of GHS-R mitigated the severity of T2D via attenuation of hyperglycemia, increased GSIS, and improvements of whole islet insulin signaling, possibly due to increased IL-1Ra activity.

Further investigations into determining the inflammatory/oxidative profile following WD/STZ treatment and the mechanisms through with GHS-R inhibition improves the outcomes are warranted. Histological analysis will allow visualization of damage or degree of de-differentiation done within pancreatic islets, as well as liver. An investigation into differences of expression/protein in key transcription factors related to dedifferentiation (PDX1, MafA, Ngn-3) of beta into alpha cells will also be pursued, to determine whether beta-cell death or de-differentiation occur in this model. Utilization of proper controls (regular diet/STZ, HFD only, each genotype on different treatment) will

provide further insight into the effects elicited by myeloid-specific GHS-R. Dissociation of islet tissue into different cell types in combination with flow cytometry and fluorescence-activated cell sorting (FACS) will allow us to specifically target beta-cells and islet macrophages for downstream analysis using single-cell RNA-seq. Furthermore, direct mechanisms of macrophage influence on islet/beta-cells will be performed using *in vitro* and *ex vivo* methods, to determine differences between genotypes and effects on insulin secretion. Finally, improvements in islet isolation from diabetic mice will be refined. Additionally, breeding LysM-Cre;Ghsr$^{f/f}$ with *db/db* mice will allow us to observe the effects of myeloid-GHS-R in a more established model of T2D.

Fig. 14

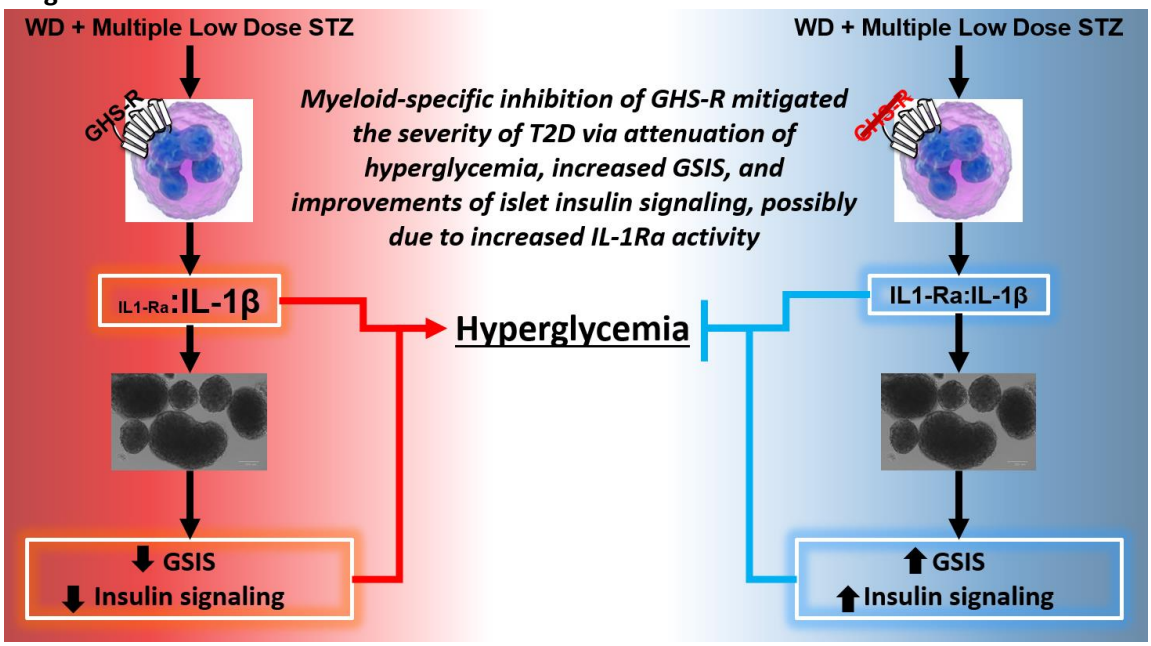

Figure 14. Summary of findings.

REFERENCES

1. Eguchi, K. and R. Nagai, *Islet inflammation in type 2 diabetes and physiology.* J Clin Invest, 2017. **127**(1): p. 14-23.

2. Westwell-Roper, C.Y., J.A. Ehses, and C.B. Verchere, *Resident macrophages mediate islet amyloid polypeptide-induced islet IL-1beta production and beta-cell dysfunction.* Diabetes, 2014. **63**(5): p. 1698-711.

3. Ehses, J.A., et al., *IL-1 antagonism reduces hyperglycemia and tissue inflammation in the type 2 diabetic GK rat.* Proc Natl Acad Sci U S A, 2009. **106**(33): p. 13998-4003.

4. Tsutsui, H., X. Cai, and S. Hayashi, *Interleukin-1 Family Cytokines in Liver Diseases.* Mediators Inflamm, 2015. **2015**: p. 630265.

5. Boni-Schnetzler, M., et al., *beta-cell-Specific Deletion of the IL-1 Receptor Antagonist Impairs beta-cell Proliferation and Insulin Secretion.* Cell Rep, 2018. **22**(7): p. 1774-1786.

6. Lin, L., et al., *Ablation of ghrelin receptor reduces adiposity and improves insulin sensitivity during aging by regulating fat metabolism in white and brown adipose tissues.* Aging Cell, 2011. **10**(6): p. 996-1010.

7. Ma, X., et al., *Ghrelin receptor regulates HFCS-induced adipose inflammation and insulin resistance.* Nutr Diabetes, 2013. **3**: p. e99.

8. Prevention, C.f.D.C.a., *National Diabetes Statistic Report*. 2017 Centers for Disease Control and Prevention, US Department of Health and Human Services: Atlanta, GA.

9. Maedler, K., et al., *Glucose-induced beta-cell production of IL-1beta contributes to glucotoxicity in human pancreatic islets.* J Clin Invest, 2002. **110**(6): p. 851-60.

10. Zonszein, J. and P.H. Groop, *Strategies for Diabetes Management: Using Newer Oral Combination Therapies Early in the Disease*. Diabetes Ther, 2016. **7**(4): p. 621-639.

11. Nath, S., S.K. Ghosh, and Y. Choudhury, *A murine model of type 2 diabetes mellitus developed using a combination of high-fat diet and multiple low doses of streptozotocin treatment mimics the metabolic characteristics of type 2 diabetes mellitus in humans.* J Pharmacol Toxicol Methods, 2017. **84**: p. 20-30.

12. Gheibi, S., K. Kashfi, and A. Ghasemi, *A practical guide for induction of type-2 diabetes in rat: Incorporating a high-fat diet and streptozotocin.* Biomed Pharmacother, 2017. **95**: p. 605-613.

13. Niu, S., et al., *Broad Infiltration of Macrophages Leads to a Proinflammatory State in Streptozotocin-Induced Hyperglycemic Mice.* Journal of immunology (Baltimore, Md. : 1950), 2016. **197**(8): p. 3293-3301.

14. Skovsø, S., *Modeling type 2 diabetes in rats using high-fat diet and streptozotocin.* Journal of diabetes investigation, 2014. **5**(4): p. 349-358.

15. He, S., et al., *Increasing glucagon secretion could antagonize the action of exogenous insulin for glycemic control in streptozocin-induced diabetic rhesus monkeys.* Exp Biol Med (Maywood), 2013. **238**(4): p. 385-91.

16. Gilbert, E.R., Z. Fu, and D. Liu, *Development of a nongenetic mouse model of type 2 diabetes.* Experimental diabetes research, 2011. **2011**: p. 416254-416254.

17. Reed, M.J., et al., *A new rat model of type 2 diabetes: The fat-fed, streptozotocin-treated rat.* Metabolism, 2000. **49**(11): p. 1390-1394.

18. Kantwerk-Funke, G., V. Burkart, and H. Kolb, *Low dose streptozotocin causes stimulation of the immune system and of anti-islet cytotoxicity in mice.* Clinical and experimental immunology, 1991. **86**(2): p. 266-270.

19. Rossini, A.A., et al., *Studies of streptozotocin-induced insulitis and diabetes.* Proceedings of the National Academy of Sciences, 1977. **74**(6): p. 2485.

20. Like, A.A. and A.A. Rossini, *Streptozotocin-induced pancreatic insulitis: new model of diabetes mellitus.* Science, 1976. **193**(4251): p. 415-7.

21. Lin, L., et al., *Ablation of ghrelin receptor reduces adiposity and improves insulin sensitivity during aging by regulating fat metabolism in white and brown adipose tissues.* 2011. **10**(6): p. 996-1010.

22. Yuan, F., et al., *Improvement of Adipose Macrophage Polarization in High-fat Diet-Induced Obese GHSR Knockout Mice.* Biomed Res Int, 2018. **2018**: p. 4924325.

23. Eguchi, K. and I. Manabe, *Macrophages and islet inflammation in type 2 diabetes.* Diabetes Obes Metab, 2013. **15 Suppl 3**: p. 152-8.

24. Fearnley, G.R., C.T. Vincent, and R. Chakrabarti, *Reduction of blood fibrinolytic activity in diabetes mellitus by insulin.* Lancet, 1959. **2**(7111): p. 1067.

25. Ogston, D. and G.M. McAndrew, *Fibrinolysis in obesity.* Lancet, 1964. **2**(7371): p. 1205-7.

26. Pradhan, A.D., et al., *C-reactive protein, interleukin 6, and risk of developing type 2 diabetes mellitus.* Jama, 2001. **286**(3): p. 327-34.

27. Thorand, B., et al., *C-reactive protein as a predictor for incident diabetes mellitus among middle-aged men: results from the MONICA Augsburg cohort study, 1984-1998.* Arch Intern Med, 2003. **163**(1): p. 93-9.

28. Shoelson, S.E., J. Lee, and A.B. Goldfine, *Inflammation and insulin resistance.* The Journal of clinical investigation, 2006. **116**(7): p. 1793-1801.

29. McArdle, M., et al., *Mechanisms of Obesity-Induced Inflammation and Insulin Resistance: Insights into the Emerging Role of Nutritional Strategies.* 2013. **4**(52).

30. Boland, B.B., C.J. Rhodes, and J.S. Grimsby, *The dynamic plasticity of insulin production in β-cells.* Molecular metabolism, 2017. **6**(9): p. 958-973.

31. Maiorino, M.I., et al., *Cooling down inflammation in type 2 diabetes: how strong is the evidence for cardiometabolic benefit?* 2017. **55**(2): p. 360-365.

32. Hundal, R.S., et al., *Mechanism by which high-dose aspirin improves glucose metabolism in type 2 diabetes.* J Clin Invest, 2002. **109**(10): p. 1321-6.

33. Fleischman, A., et al., *Salsalate improves glycemia and inflammatory parameters in obese young adults.* Diabetes Care, 2008. **31**(2): p. 289-94.

34. Su, D., et al., *FoxO1 links insulin resistance to proinflammatory cytokine IL-1beta production in macrophages.* Diabetes, 2009. **58**(11): p. 2624-33.

35. Rosenson, R.S., et al., *Fenofibrate reduces fasting and postprandial inflammatory responses among hypertriglyceridemia patients with the metabolic syndrome.* Atherosclerosis, 2008. **198**(2): p. 381-8.

36. Rautio, K., et al., *Rosiglitazone treatment alleviates inflammation and improves liver function in overweight women with polycystic ovary syndrome: a randomized placebo-controlled study.* Fertil Steril, 2007. **87**(1): p. 202-6.

37. Hotamisligil, G.S., *Inflammation and metabolic disorders.* Nature, 2006. **444**(7121): p. 860-7.

38. Chen, L., et al., *Mechanisms Linking Inflammation to Insulin Resistance %J International Journal of Endocrinology.* 2015. **2015**: p. 9.

39. Böni-Schnetzler, M. and M.Y. Donath, *How biologics targeting the IL-1 system are being considered for the treatment of type 2 diabetes.* British journal of clinical pharmacology, 2013. **76**(2): p. 263-268.

40. Hardaway, A.L. and I. Podgorski, *IL-1beta, RAGE and FABP4: targeting the dynamic trio in metabolic inflammation and related pathologies.* Future Med Chem, 2013. **5**(10): p. 1089-108.

41. Grant, R.W. and V.D. Dixit, *Mechanisms of disease: inflammasome activation and the development of type 2 diabetes.* Front Immunol, 2013. **4**: p. 50.

42. Weber, A., P. Wasiliew, and M. Kracht, *Interleukin-1 (IL-1) Pathway.* 2010. **3**(105): p. cm1-cm1.

43. Maedler, K., et al., *Interleukin-1 beta targeted therapy for type 2 diabetes.* Expert Opin Biol Ther, 2009. **9**(9): p. 1177-88.

44. Maedler, K., et al., *Interleukin-Targeted Therapy for Metabolic Syndrome and Type 2 Diabetes*, in *Diabetes - Perspectives in Drug Therapy*, M. Schwanstecher, Editor. 2011, Springer Berlin Heidelberg: Berlin, Heidelberg. p. 257-278.

45. Kim, O.K., W. Jun, and J. Lee, *Mechanism of ER Stress and Inflammation for Hepatic Insulin Resistance in Obesity.* Annals of Nutrition and Metabolism, 2015. **67**(4): p. 218-227.

46. Huang, X., et al., *The PI3K/AKT pathway in obesity and type 2 diabetes.* International journal of biological sciences, 2018. **14**(11): p. 1483-1496.

47. Cantley, J., et al., *Pancreatic deletion of insulin receptor substrate 2 reduces beta and alpha cell mass and impairs glucose homeostasis in mice.* Diabetologia, 2007. **50**(6): p. 1248-56.

48. Bernal-Mizrachi, E., et al., *Islet beta-cell expression of constitutively active Akt1/PKB alpha induces striking hypertrophy, hyperplasia, and hyperinsulinemia.* J Clin Invest, 2001. **108**(11): p. 1631-8.

49. Fujimoto, K. and K.S. Polonsky, *Pdx1 and other factors that regulate pancreatic β-cell survival.* 2009. **11**(s4): p. 30-37.

50. Brissova, M., et al., *Reduction in pancreatic transcription factor PDX-1 impairs glucose-stimulated insulin secretion.* J Biol Chem, 2002. **277**(13): p. 11225-32.

51. Swisa, A., B. Glaser, and Y. Dor, *Metabolic Stress and Compromised Identity of Pancreatic Beta-cells.* Frontiers in genetics, 2017. **8**: p. 21-21.

52. Xiao, X. and G.K. Gittes, *Concise Review: New Insights Into the Role of Macrophages in β-Cell Proliferation.* Stem cells translational medicine, 2015. **4**(6): p. 655-658.

53. Dror, E., et al., *Postprandial macrophage-derived IL-1β stimulates insulin, and both synergistically promote glucose disposal and inflammation.* Nature Immunology, 2017. **18**: p. 283.

54. Meshkani, R. and K. Adeli, *Hepatic insulin resistance, metabolic syndrome and cardiovascular disease.* Clinical Biochemistry, 2009. **42**(13): p. 1331-1346.

55. Donath, M.Y. and S.E. Shoelson, *Type 2 diabetes as an inflammatory disease.* Nature Reviews Immunology, 2011. **11**: p. 98.

56. Boni-Schnetzler, M., et al., *Free fatty acids induce a proinflammatory response in islets via the abundantly expressed interleukin-1 receptor I.* Endocrinology, 2009. **150**(12): p. 5218-29.

57. Larsen, C.M., et al., *Sustained effects of interleukin-1 receptor antagonist treatment in type 2 diabetes.* Diabetes Care, 2009. **32**(9): p. 1663-8.

58. Boni-Schnetzler, M., et al., *Increased interleukin (IL)-1beta messenger ribonucleic acid expression in beta -cells of individuals with type 2 diabetes and regulation of IL-1beta in human islets by glucose and autostimulation.* J Clin Endocrinol Metab, 2008. **93**(10): p. 4065-74.

59. Barshes, N.R., S. Wyllie, and J.A. Goss, *Inflammation-mediated dysfunction and apoptosis in pancreatic islet transplantation: implications for intrahepatic grafts.* J Leukoc Biol, 2005. **77**(5): p. 587-97.

60. Sauter, N.S., et al., *The antiinflammatory cytokine interleukin-1 receptor antagonist protects from high-fat diet-induced hyperglycemia.* Endocrinology, 2008. **149**(5): p. 2208-18.

61. Peiró, C., et al., *IL-1β Inhibition in Cardiovascular Complications Associated to Diabetes Mellitus.* 2017. **8**(363).

62. Smith, R.G., H. Jiang, and Y. Sun, *Developments in ghrelin biology and potential clinical relevance.* Trends in Endocrinology & Metabolism, 2005. **16**(9): p. 436-442.

63. Ma, X., et al., *Ablation of ghrelin receptor in leptin-deficient ob/ob mice has paradoxical effects on glucose homeostasis when compared with ablation of ghrelin in ob/ob mice.* 2012. **303**(3): p. E422-E431.

64. Muller, T.D., et al., *Ghrelin.* Mol Metab, 2015. **4**(6): p. 437-60.

65. Sun, Y., et al., *Ghrelin stimulation of growth hormone release and appetite is mediated through the growth hormone secretagogue receptor.* Proceedings of the National Academy of Sciences of the United States of America, 2004. **101**(13): p. 4679-4684.

66. Sun, Y., R.G. Smith, and J.M. Garcia, *Ghrelin and Growth Hormone Secretagogue Receptor Expression in Mice during Aging.* Endocrinology, 2007. **148**(3): p. 1323-1329.

67. Damian, M., et al., *High constitutive activity is an intrinsic feature of ghrelin receptor protein: a study with a functional monomeric GHS-R1a receptor reconstituted in lipid discs.* J Biol Chem, 2012. **287**(6): p. 3630-41.

68. Sun, Y., et al., *Characterization of adult ghrelin and ghrelin receptor knockout mice under positive and negative energy balance.* Endocrinology, 2008. **149**(2): p. 843-850.

69. Lin, L., et al., *Ghrelin receptor regulates adipose tissue inflammation in aging.* Aging (Albany NY), 2016. **8**(1): p. 178-91.

70. Amati, F., et al., *Physical inactivity and obesity underlie the insulin resistance of aging.* Diabetes Care, 2009. **32**(8): p. 1547-9.

71. Ahima, R.S.J.N.m., *Connecting obesity, aging and diabetes.* 2009. **15**(9): p. 996.

72. Lenzen, S., *The mechanisms of alloxan- and streptozotocin-induced diabetes.* Diabetologia, 2008. **51**(2): p. 216-226.

73. Sasidharan, S.R., et al., *An Experimental Approach for Selecting Appropriate Rodent Diets for Research Studies on Metabolic Disorders %J BioMed Research International.* 2013. **2013**: p. 9.

74. Gheibi, S., K. Kashfi, and A. Ghasemi, *A practical guide for induction of type-2 diabetes in rat: Incorporating a high-fat diet and streptozotocin.* Biomedicine & Pharmacotherapy, 2017. **95**: p. 605-613.

75. Lukic, M.L., S. Stosic-Grujicic, and A. Shahin, *Effector mechanisms in low-dose streptozotocin-induced diabetes.* Dev Immunol, 1998. **6**(1-2): p. 119-28.

76. Novikova, L., et al., *Variations in Rodent Models of Type 1 Diabetes: Islet Morphology %J Journal of Diabetes Research.* 2013. **2013**: p. 13.

77. Ishimoto, T., et al., *High-fat and high-sucrose (western) diet induces steatohepatitis that is dependent on fructokinase.* Hepatology, 2013. **58**(5): p. 1632-43.

78. Agrawal, N.K. and S. Kant, *Targeting inflammation in diabetes: Newer therapeutic options.* World journal of diabetes, 2014. **5**(5): p. 697-710.

79. Melloul, D., *Role of NF-κB in β-cell death.* 2008. **36**(3): p. 334-339.

80. Fonseca, S.G., et al., *Endoplasmic reticulum stress in beta-cells and development of diabetes.* Curr Opin Pharmacol, 2009. **9**(6): p. 763-70.

81. Meier, J.J., *Beta-cell mass in diabetes: a realistic therapeutic target?* Diabetologia, 2008. **51**(5): p. 703-13.

82. Winzell, M.S. and B. Ahrén, *The High-Fat Diet–Fed Mouse.* A Model for Studying Mechanisms and Treatment of Impaired Glucose Tolerance and Type 2 Diabetes, 2004. **53**(suppl 3): p. S215-S219.

83. Zhang, M., et al., *The Characterization of High-Fat Diet and Multiple Low-Dose Streptozotocin Induced Type 2 Diabetes Rat Model %J Experimental Diabetes Research.* 2008. **2008**: p. 9.

84. da Silva, R.C.Q., et al., *Insulin resistance, β-cell function, and glucose tolerance in Brazilian adolescents with obesity or risk factors for type 2 diabetes mellitus.* Journal of Diabetes and its Complications, 2007. **21**(2): p. 84-92.

85. McNelis, Joanne C. and Jerrold M. Olefsky, *Macrophages, Immunity, and Metabolic Disease.* Immunity, 2014. **41**(1): p. 36-48.

86. Furman, B.L., *Streptozotocin-Induced Diabetic Models in Mice and Rats.* Curr Protoc Pharmacol, 2015. **70**: p. 5.47.1-20.

87. Sun, Y., J.M. Garcia, and R.G. Smith, *Ghrelin and growth hormone secretagogue receptor expression in mice during aging.* Endocrinology, 2007. **148**(3): p. 1323-9.

88. Grant, C.W., et al., *Development of standardized insulin treatment protocols for spontaneous rodent models of type 1 diabetes.* Comparative medicine, 2012. **62**(5): p. 381-390.

89. Liu, W., et al., *Hypoglycemic, hypolipidemic and antioxidant effects of Sarcandra glabra polysaccharide in type 2 diabetic mice.* Food Funct, 2014. **5**(11): p. 2850-60.

90. Gosmain, Y., M.H. Masson, and J. Philippe, *Glucagon: the renewal of an old hormone in the pathophysiology of diabetes.* J Diabetes, 2013. **5**(2): p. 102-9.

91. Lin, H.V. and D. Accili, *Hormonal regulation of hepatic glucose production in health and disease.* Cell Metab, 2011. **14**(1): p. 9-19.

92. Wallace, T.M., J.C. Levy, and D.R. Matthews, *Use and Abuse of HOMA Modeling.* 2004. **27**(6): p. 1487-1495.

93. van Dijk, T.H., et al., *A novel approach to monitor glucose metabolism using stable isotopically labelled glucose in longitudinal studies in mice.* Lab Anim, 2013. **47**(2): p. 79-88.

94. Vogeser, M., et al., *Fasting serum insulin and the homeostasis model of insulin resistance (HOMA-IR) in the monitoring of lifestyle interventions in obese persons.* Clin Biochem, 2007. **40**(13-14): p. 964-8.

95. Nagaraj, V., et al., *Elevated Basal Insulin Secretion in Type 2 Diabetes Caused by Reduced Plasma Membrane Cholesterol.* Molecular endocrinology (Baltimore, Md.), 2016. **30**(10): p. 1059-1069.

96. Liu, S., et al., *Effects of vaspin on pancreatic β cell secretion via PI3K/Akt and NF-κB signaling pathways.* PLOS ONE, 2017. **12**(12): p. e0189722.

97. Nackiewicz, D., et al., *Islet macrophages are the primary islet source of IGF-1 and improve glucose homeostasis following pancreatic beta-cell death.* 2018: p. 480368.

98. Van Haeften, T.W. and T.B. Twickler, *Insulin-like growth factors and pancreas beta-cells.* 2004. **34**(4): p. 249-255.

99. Withers, D.J., et al., *Disruption of IRS-2 causes type 2 diabetes in mice.* Nature, 1998. **391**(6670): p. 900-4.

100. Kulkarni, R.N., et al., *Altered function of insulin receptor substrate-1-deficient mouse islets and cultured beta-cell lines.* J Clin Invest, 1999. **104**(12): p. R69-75.

101. Thorens, B.J.D., *GLUT2, glucose sensing and glucose homeostasis.* 2015. **58**(2): p. 221-232.

102. Shankar, E., et al., *Inflammatory Signaling Involved in High-Fat Diet-induced Prostate Diseases.* Journal of urology and research, 2015. **2**(1): p. 1018.

103. Akash, M.S.H., K. Rehman, and A. Liaqat, *Tumor Necrosis Factor-Alpha: Role in Development of Insulin Resistance and Pathogenesis of Type 2 Diabetes Mellitus.* J Cell Biochem, 2018. **119**(1): p. 105-110.

104. Kristiansen, O.P. and T. Mandrup-Poulsen, *Interleukin-6 and diabetes: the good, the bad, or the indifferent?* Diabetes, 2005. **54 Suppl 2**: p. S114-24.

105. Godoy-Matos, A.F.J.D. and M. Syndrome, *The role of glucagon on type 2 diabetes at a glance.* 2014. **6**(1): p. 91.

106. Srinivasan, K., et al., *Combination of high-fat diet-fed and low-dose streptozotocin-treated rat: A model for type 2 diabetes and pharmacological screening.* Pharmacological Research, 2005. **52**(4): p. 313-320.

107. Esser, N., et al., *Inflammation as a link between obesity, metabolic syndrome and type 2 diabetes.* Diabetes Res Clin Pract, 2014. **105**(2): p. 141-50.

108. Aschner, P., *Metabolic syndrome as a risk factor for diabetes.* Expert Rev Cardiovasc Ther, 2010. **8**(3): p. 407-12.

109. Gerich, J.E., *Is Reduced First-Phase Insulin Release the Earliest Detectable Abnormality in Individuals Destined to Develop Type 2 Diabetes?* 2002. **51**(suppl 1): p. S117-S121.

110. Wang, W.-T., et al., *Effects of acute and chronic hyperglycemia on the neurochemical profiles in the rat brain with streptozotocin-induced diabetes detected using in vivo ^{1}H MR spectroscopy at 9.4 T.* Journal of neurochemistry, 2012. **121**(3): p. 407-417.

111. Weber, A., P. Wasiliew, and M. Kracht, *Interleukin-1 (IL-1) pathway.* Sci Signal, 2010. **3**(105): p. cm1.

112. Sandberg, J.O., et al., *Interleukin-1 receptor antagonist prevents low dose streptozotocin induced diabetes in mice.* Biochem Biophys Res Commun, 1994. **202**(1): p. 543-8.